Carbon isotope chemostratigraphy of the Late Silurian Lau Event, Gotland, Sweden

Hani Younes

Dissertations in Geology at Lund University,
Master's thesis, no 318
(45 hp/ECTS credits)

Department of Geology
Lund University
2012

Carbon isotope chemostratigraphy of the Late Silurian Lau Event, Gotland, Sweden

Master's thesis

Hani Younes

Department of Geology
Lund University

2012

Contents

1- Introduction.....3

2- Geological setting and stratigraphy.....4

3- The Lau Event.....7

4- Material and methods.....10

5- Results.....13

5-1 sedimentary facies of the Uddvide-1 drill core.....13

5-2 sedimentary facies of the Ronehamn-1 drill core.....15

5-3 Carbon isotope chemostratigraphy.....18

6- Discussion.....21

6-1 Chemostratigraphic model for the Lau Event.....21

6-2 Chemostratigraphical correlations.....24

6-2-1 Uddvide-1, Gotland vs COG north-eastern Australia.....24

6-2-2 Uddvide-1, Gotland vs Baltica.....25

6-2-3 Uddvide-1, Gotland vs Bohimia.....28

6-2-4 Uddvide-1, Gotland vs Laurentia.....29

7- Conclusions.....31

8- Acknowledgments.....32

9- References.....33

10– Appendix.....36

Carbon isotope chemostratigraphy of the Late Silurian Lau Event, Gotland, Sweden

HANI YOUNES[1]

Younes, H., 2012: Carbon isotope chemostratigraphy of the Late Silurian Lau Event, Gotland, Sweden. *Dissertations in Geology at Lund University*, No. 318., 40 pp. 45 hp (45 ECTS credits).

Abstract: The positive $\delta^{13}C$ excursion associated with the Late Silurian Lau Event (approximately 420 Ma) is recognized globally and considered to be one of the most prominent carbon isotope excursions of the Phanerozoic. Its maximum values are exceeded only by values from the Proterozoic. Over the last years the Lau Event has been studied in great detail on the island of Gotland, Sweden (Baltica palaeocontinent). These studies include lithological successions and high-resolution conodont biostratigraphy, as well as $\delta^{13}C$ chemostratigraphy. For these reasons, Gotland is considered the standard classical model for studying the Lau Event. The purpose of the present study is to produce the first continuous, high-resolution $\delta^{13}C$ stratigraphy across the stratigraphic range of the event. The $\delta^{13}C$ record is based on two drill cores (Uddvide-1 and Ronehamn-1) and work as a standard model for global correlation of the event. The generated profiles have high positive peak values of 8.03 ‰ and 9.01 ‰ respectively in Uddvide-1 and Ronehamn-1 drill cores. Both profiles have the typical model of the Lau Event consisting of rising limb, plateau and falling limb. The correlation not only improves the knowledge on Ludlow stratigraphy but also helps to understand the evolution of climate, marine ecosystems and depositional environment during the Ludfordian. In doing so, the cause of this high positive $\delta^{13}C$ excursion will be better understood.

Keywords: Silurian, Lau Event, extinction, Gotland, carbon isotope excursion, conodonts, high-resolution correlation, microbial resurgence.

Supervisors: Mikael Calner and Per Ahlberg

[1]*Department of Geology, Lund University, Sölvegatan 12, SE-223 62 Lund, Sweden; haniyounes9@gmail.com*

1- Introduction

Major and minor extinction events have dramatically affected biodiversity throughout the history of life on Earth (Sepkoski et al., 1981). Studying the causes and mechanism of these events forms the basis of understanding the diversification of taxa and evolution of life. Many studies on stable carbon isotope chemostratigraphy of sedimentary successions of various ages were published over the last fifteen years. These studies have unequivocally shown that most ancient crises in marine faunas are accompanied by anomalies in the relationshion between ^{12}C and ^{13}C, shown as anomalies in $\delta^{13}C$. In the Palaeozoic these excursions are positive and normally range from one to a few per mil. Most of them are excellent for intercontinental correlation of sedimentary packages, e.g. the Guttenberg Carbon Isotope Excursion (GICE; Saltzman 2001) and the Hirnantian Carbon Isotope Excursion (HICE; Bergström et al. 2006) in the Ordovician, and the Ireviken, Mulde and Lau excursions in the Silurian (Calner 2008). The cause(s) for the many carbon cycle anomalies in the Palaeozoic is not understood although several models involving the ocean-atmosphere system have been proposed (Cramer et al. 2006; Eriksson and Calner 2008). The similarity in their geochemical, paleontological, and sedimentological characteristics, however, implies a singular causing mechanism (Munnecke et al., 2003). The Silurian Period (444-416 Ma) was for long time thought to be a stable period in Earth history with respect to dramatic changes in the ocean-atmospheric system. Recurrent fossil faunal anomalies and distinct positive carbon isotope excursions, however, have now shown it to be one of the most variable periods of the Phanerozoic (Cramer and Saltzman 2005; Calner 2008). The integrated stable

isotopes and faunal changes data/models obtained from different palaeocontinents have instead transformed the Silurian Period to be a key object for studies and researches on climate change, environmental and oceanographic perturbations (Lehnert et al. 2006). The most prominent $\delta^{13}C$ excursion of the Silurian, and surprisingly little studied, is that associated with the Late Silurian Lau Event. This is a minor extinction event and faunal turnover that was first recognised and named by Jeppsson (1987, 1990, and 1993). It is the last of the three major ecological turnovers and biotic events that occurred during the Silurian Period (Jeppsson 1990; 1998; summarised by Calner 2008). It affected conodonts severely but had less effect on graptolites (Jeppsson and Aldridge 2000). Several other groups have been analysed with respect to the Lau Event, including acritarchs, chitinozoans, corals, brachiopods, ostracodes, trilobites, tentaculitides, fishs, and polychaetes (Eriksson 2004; Eriksson and Claner 2008). Perhaps most prominent is the major anomaly in the global carbon cycle that is associated with the event. This perturbation, which was first detailed from southernmost Sweden (Wigforss -Lange 1999) and which has a magnitude of more than 10 per mil in some areas, is considered the largest in the whole Phanerozoic and the second largest in Earth's history (Munnecke at al. 2003; Barrick 2010). The carbon isotope excursion has been detected in several different palaeocontinents (Fig. 4 and Table 1). These excursions attain maximum values ranging from 3 ‰ in Southern Laurenthia (Barrick 2010), 9 ‰ on Gotland (this study), 11 ‰ from southern Sweden (Wigforss-Lange 1999) and even up to 12 ‰ in Queensland Australia (Jeppsson et al. 2007). Since the Lau Event was first recognised, and is stratigraphically well defined on Gotland (Figs. 1 and 2), this island may function as the type area for the event (Calner 2005; Jeppsson et al. 2006; Calner 2008; Eriksson and Calner 2008). The abundant and well preserved fossil faunas here serve in studying the Lau Event and allow precise high-resolution correlations by means of biostratigraphy as well chemostratigraphical data obtained from $\delta^{13}C$ analysis (e.g. Samtleben et al. 2000; Calner et al. 2006; Lehnert et al. 2010). Since Gotl-nd is considered a classical model for studying the Lau Event (Calner 2005; Jeppsson et al. 2006;Calner 2008; Eriksson and Calner 2008), it is worth mentioning that many researchers have correlated or at least compared their $\delta^{13}C$ results in combination with lithofacies and faunal changes to its equivalent sequences of Gotland (e.g. Saltzman 2002; Jeppsson et al. 2007; Kozlowski and Munnecke 2012). The main objective of this study is to establish a continuous, high-resolution $\delta^{13}C$ profile across the Lau Event based on the successions of Uddvide-1 drill core (in correlation with the Ronehamn-1 drill core). This curve will function as a model for correlation of the strata with coeval successions in other palaeocontinents in order to investigate the morphological variation of this exceptionally strong positive $\delta^{13}C$ excursion and the stratigraphic completeness of various Ludfordian sections. The study is therefore a first attempt to correlate several successions from widely separated palaeocontinents of Lau Event.

2- Geological setting and stratigraphy

The uppermost Llandovery through Ludlow strata on Gotland was formed within the Baltic Basin, which was a warm and shallow epicontinental sea covering large parts of southern Scandinavia and the East Baltic area (Fig. 1A). The Baltic Basin was affected by three tectonic developments, the Caledonian, Variscian and Alpine orogenesis (Poprawa et al. 1999). The Caledonian orogeny and the accretion of Avalonia have been affecting the southwestern margins from the Late Ordovician and onwards (Eriksson and Calner 2008). The Rheic ocean and rifted Gondwana terranes were located to the south of Baltic Basin in Late Silurian (Fig. 1A). Metamorphism and strong folding have no clear effect on strata of Gotland (Jeppsson 2005). The Uddvide-1 drill core is located in deeper subtidal carbonate platform comparing to Ronehamn-1 drill core (Calner 2008)(Fig. 3A). The succession on Gotland yields reef and stratified limestone, marlstone, and to a lesser extent fine-grained siliclastic deposits. The stratigraphical subdivision of the succession was introduced by Hede (1921 and 1925, summarized in English in 1960).

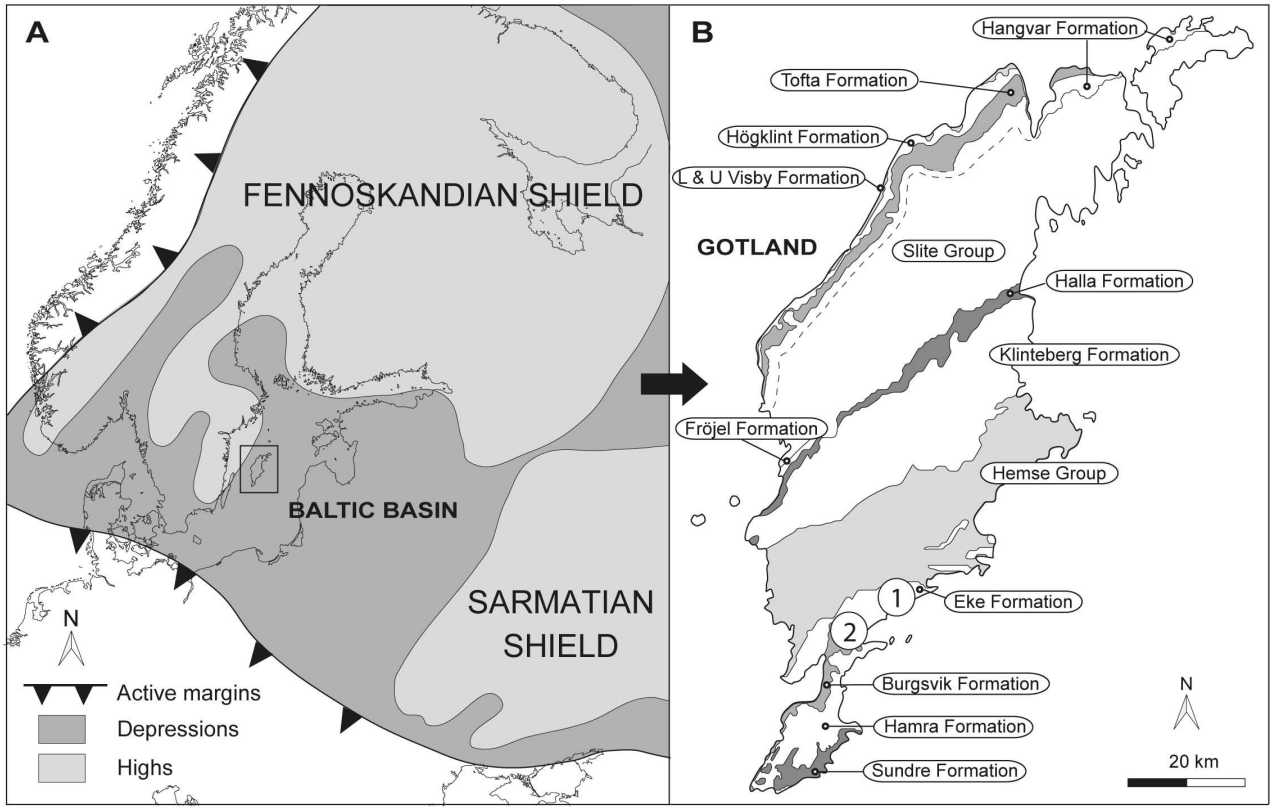

Fig. 1. A Silurian palaeogeography of Baltica and the East Baltic area with location of Gotland within the square (modified from Baarli et al. 2003). **B** Stratigraphical units of Gotland with the location of drill cores indicated. (1) Ronehamn-1 drill core, (2) Uddvide-1 drill core.

The most recent stratigraphic revision was presented by Jeppsson et al. (2006) (Figs. 1B, 2 and 3B). The oldest strata considered for the present study belong to the uppermost part of the När Formation of the Hemse Group. This succession is ca 13-14 m thick in the Uddvide-1 drill core and ca 13.5 m in Ronehamn-1 drill core. The strata consist of interbedded skeletal mudstone-wackestone and marl and it is charcterised by diverse assemblage of fossils. The depositional environment has been interpreted as fairly deep below wave base seaward of a reef barrier (Eriksson and Calner 2008). Whereas Botvide Member is absent in the Uddvide-1 core, it occupies the uppermost decimeters of Hemse Group in Ronehamn-1 drill core. This member is charcterised by coquinas of the brachiopod *Dayia navicula* in a slightly dolomitic mudstone with rare limestone beds (Jeppsson 2005). När Formation is separated from the overlying Eke Formation in the eastern part of the outcrop belt by a stratigraphical hiatus (Manten 1971; Cherns 1982; Eriksson and Calner 2008). The Eke Formation (≈ 15 m thick in Uddvide-1 and ≈ 12 m thick in Ronehamn-1) is charcterised by high abundance of oncoids (*Rothpletzella* and *Wetheredella*), which have been used as the main defining charcater of the formation (Jeppsson 2005). The formation comprises argillaceous, silty crinoidal wackestone-packstone and oncoidal wackestone-packstone with interbedded marl. The formation yield an impoverished conodont fauna and rare graptolites (Jeppsson 2005). Crinoid debris are the most common fossils represented in local reef limestones within the Eke Formation (Manten 1971). The overlying ca 32.5 m thick Burgsvik Formation comprises quartz sandstone, siltstone and shale overlain by a thin cap of oolitic limestone in the Uddvide-1 core. In the Ronehamn-1 drill core, only

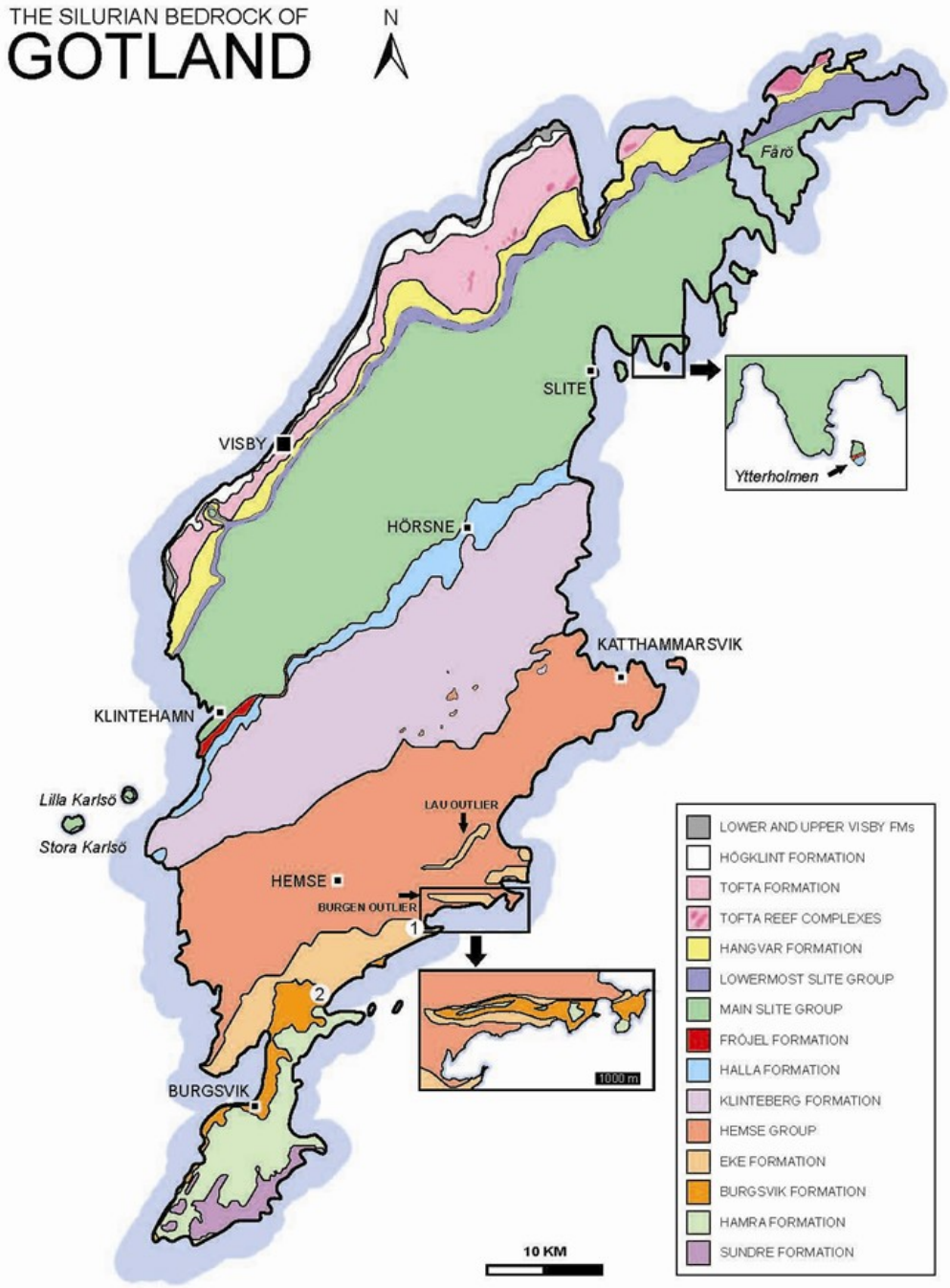

Fig. 2. The Geological map of Gotland showing the major Hede's subdivision and locations of 1- Ronehamn-1 and 2- Uddvide-1 drill cores (Jeppsson 2005a).

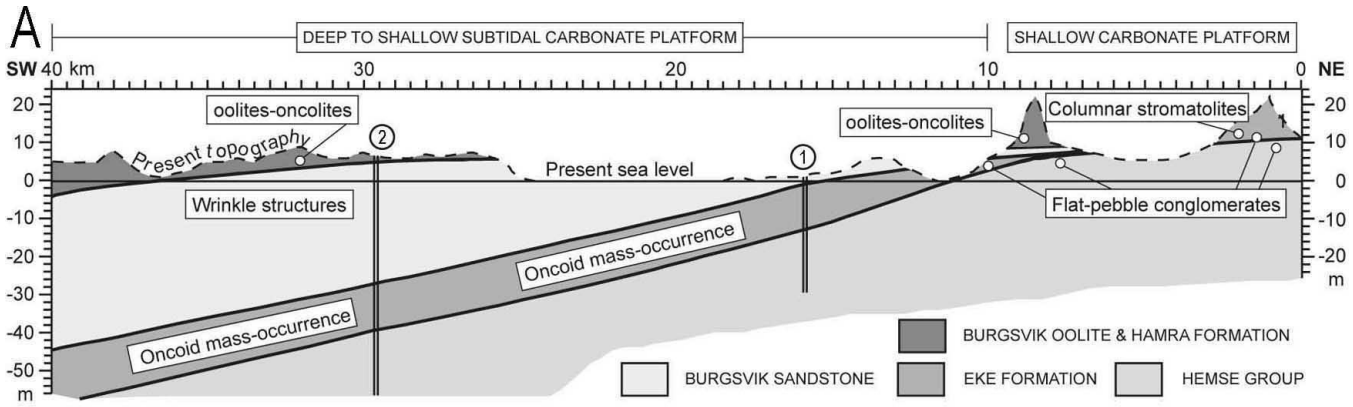

B

Age	Conodont zones	Stratigraphy
Ludfordian	*Ozarkodina snajdri* Zone	Hamra Fm.
		Burgsvik Fm.
	Icriodontoid Zone: upper	Eke Fm: upper
	Icriodontoid Zone: middle	Eke Fm: middle
	Icriodontoid Zone: lower	Eke Fm: lower
	LAD *P. siluricus*	Botvide Member
	Polygnathoides siluricus Zone	När Fm.

Fig. 3 **A** Cross section showing the formations involved in Lau Event and penetrated by the two studied cores, (1) Ronehamn-1, (2) Uddvide-1, and spatial distribution of microbial fossils and anachronistic facies. Modified from Calner (2005). **B** Conodont zonation of Ludfordian Age, Late Silurian after Jeppsson (2006).

the two basal metres of the Burgsvik Formation is preserved. The uppermost portion of the Burgsvik Formation in the Uddvide-1 drill core constitutes the thin Burgsvik Oolite Member. The ooids have originated by precipitation from marine waters supersaturated with respect to calcium carbonate (cf. Bosence and Wilson 2003).

3- The Lau Event

The Lau Event started at the beginning of Ludfordian Stage and was accompanied, in the Baltic basin, by substantial sea level changes and a major positive carbon isotope excursion (Eriksson and Calner 2008). Among marine groups, especially conodonts were affected during the event and only six out of 23 species present in pre-extinction strata survived. None of the platform-equipped conodonts survived during the event. Conodonts are a reliable tool for stratigraphic correlation in Silurian shallow-water successions, and since this was the most affected group during the event, conodonts are considered key fossils for a reliable biostratigraphical identification of the Lau Event. The detailed conodont zonation for the Ludlow was developed and revised over the last few years by Jeppsson (2005, 2006; Figs. 3A and 5). The extinction of the widespread zone fossil *Polygnathoides siluricus* is considered a mark for the beginning of the Lau Event (Jeppsson

2005). The Icriodontid zone represents the lowest diversity conodont fauna that prevailed during the event, whereas a recovery is seen in the *O. snajdri* Zone. Platform conodonts were very diverse in the main part of *P. siluricus* Zone, but they suffered rapid stepwise extinctions in the upper *P. siluricus* and *O. excavata* faunal subzones, corresponding to the base of the Botvide Member of the När Formation (Jeppsson 1998; Jeppsson 2005). The next younger zone, the Icriodontid Zone, corresponds to the Eke Formation. The name of the zone was introduced by Jeppsson (2005) for the widely recognised interval of strongly impoverished faunas that followed *P. siluricus* extinction. Eke Formation is subdivided into three sub-units; lower, middle and upper Eke, and each of these sub-unites coincides with one of the Icriodontid subzones. The lowerEke coincides with the Lower Icriodontid conodont subzone. The middle Eke coincides with the Middle Icriodontid conodont subzone, its base is defined by the re-occurrence of a slender form of *P. equicostatus*. The upper Eke coincides with the Upper Icriodontid conodont subzone, in which only one single conodont species (*Panderodus equicostatus* on Gotland and *Ozarkodina scanica* in Skåne), has survived from the past stages of extinction. This species is strongly dominant (Jeppsson 1998; Jeppsson and Aldridge 2000; Jeppsson 2005). In the recovery stage at the end of the event there is a moderate diversity in the *O. snajdri* conodont Zone, which corresponds to the lowermost part of the Burgsvik Formation (Jeppsson 1998; Jeppsson 2005). The graptolite fauna experienced the same development as well; they were diverse With *N. kozlowski* in the main part of the När Formation (upper part of the Hemse Group).

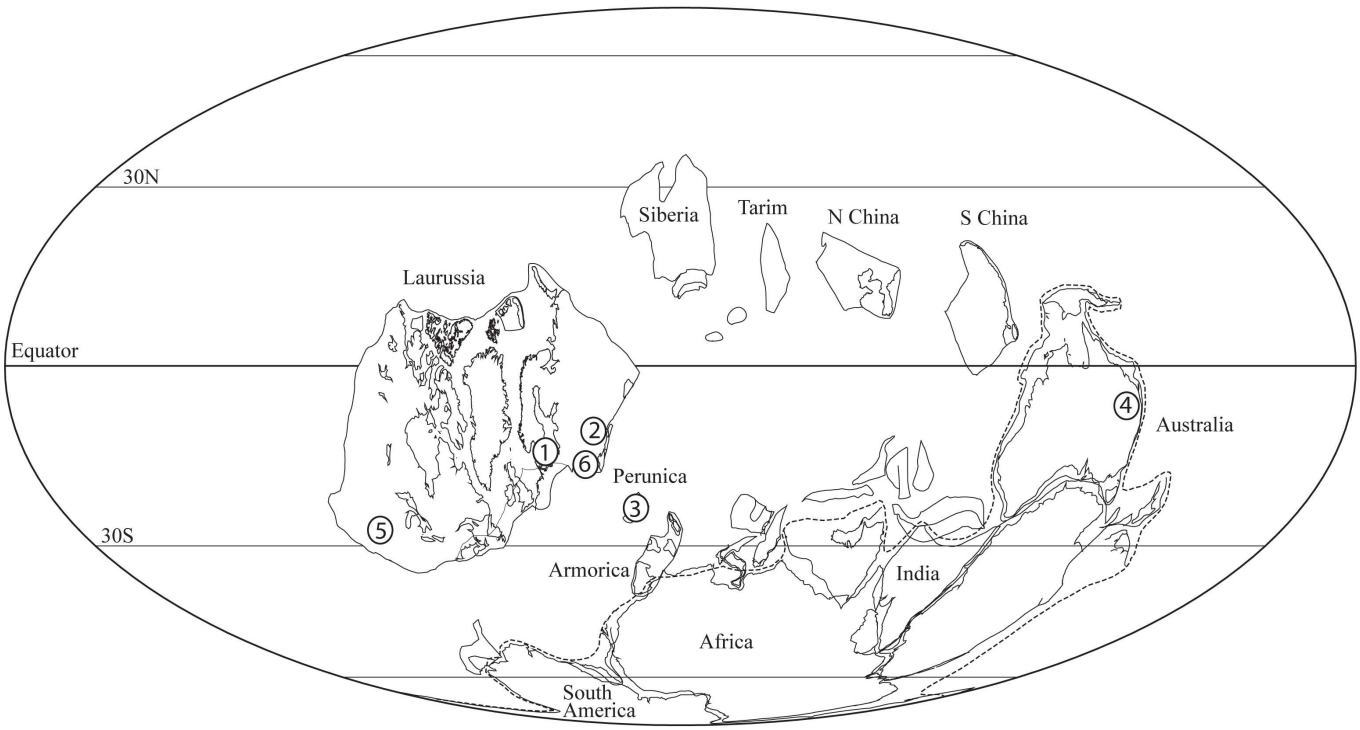

Fig. 4. Palaeogeographical distribution for published records of the positive carbon isotope excursion during the late Silurian (Ludfordian) Lau Event. Some of the locations represent more than one published report and a number of sections. (1) Gotland, Sweden, the two drill cores analysised in this study, (2) Eastern Baltica (Kaljo 2007), (3) The Prague Basin (Lehnert et al. 2007a,b), Palaeogeographic reconstruction from Cocks and Totsvik (2002). (4) Queensland Australia (Jeppsson at al. 2007), (5) Laurentia palaeocontinent, Oklahoma, Tennesse and Missori, United States (Barrick 2010). (6) Southern Baltica (Kozlowski 2012).

In Eke Formation we have an impoverished fauna, followed by a moderately diverse fauna with *Pm. latilobus* in the recovery stage in the lowermost part of Burgsvik Sandstone Member (Jeppsson 2005; Fig. 5). Also the marine sedimentary facies changed substantially during the event, implying rather profound environmental changes to the carbonate platform ecosystem (Calner 2005). Tropical shallow-marine carbonate platforms are built by rapidly calcifying organisms (Bosence and Wilson 2003). These organims are very sensitive for marine environmental changes. According to recent studies of the strata on Gotland, major changes in composition and structure of carbonate platforms were associated with the event (Jeppsson 2003; Calner et al. 2004; Calner 2005; Calner and Eriksson 2006). Most notable, the sediments deposited during and shortly after Lau Event are characterised by anachronistic facies, which those that prevailed in earlier times in Earth history, particularly in the Pre-Camberian Era (Schubert and Bottjer 1992; Hagadorn and Bottjer 1997; Whalen et al. 2002; Pruss et al. 2004; Sheehan and Harris 2004; Calner 2005). Flat-pebble conglomerates, stromatolites, oncolites, oolites and wrinkle structures are prominent in the Eke and Burgsvik Formations (Calner 2005). The lowermost part of the Eke Formation, at the boundary with the Botvide Member, is characterised by the existence of flat-pebble conglomerates. The abundance of crinoids and oncoids in Eke Formation indicates a warm-water shallow marine environment. In both drill cores, the abundance of oncoids (*Rothplezella* and *Wetherdella*) is high (Fig. 7C) in addition to well preserved brachiopods (Fig. 7B) in the argillaceous Eke Formation. *Rothpletzella* with thick cortices are the most abundant oncoids in Eke Formation (Calner 2005).

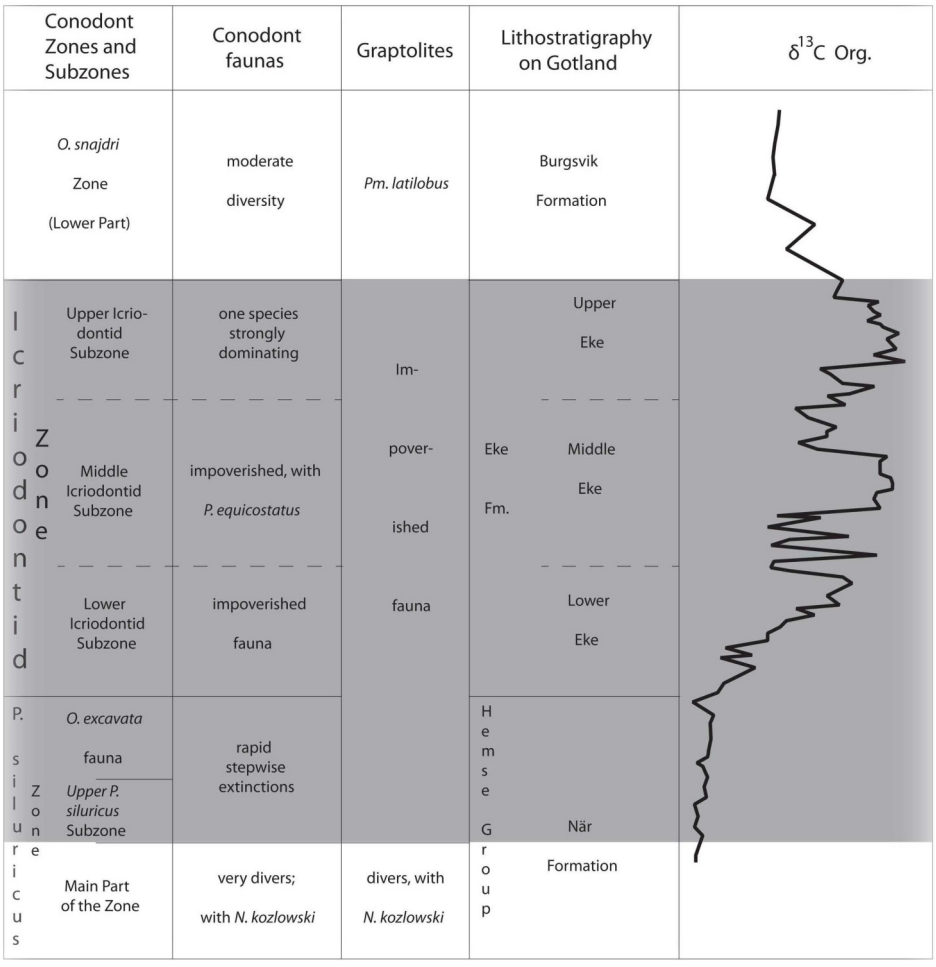

Fig. 5. Conodont and graptolites zones and subzones and corresponding formations and subformations, the shadowed part represents Lau Event ($\delta^{13}C$ curve was obtained from this study and the faunal changes are modified from Jeppsson 2005).

Table 1. Locations of previous Lau Event studies including carbon isotopes analyses.

Location	´ Formation	Peak Values	Key Reference
Baltica			
Gotland	*Eke Formation*	*9.01 ‰*	*this paper*
Poland	*Winnica Formation*	*8.89 ‰*	*Kozlowski 2012*
Podolia-Ukraine	*Rykhta andPrigorodok Fm.*	*4.3 ‰*	*Kaljo et al. 2007*
Lithuania	*Mituva Formation*	*8.17 ‰*	*Martma et al. 2005*
Northern Europe			
Czeck Republic	*Upper Kopanina Formation*	*8‰*	*Lehnert 2007*
North America			
Southern Oklahoma	*Henryhouse Formation*	*3.66‰*	*Barrick 2010*
South-Eastern Missori	*Bainbridge Formation*	*5.41‰*	*Barrick 2010*
Western Tennessee	*Brownsport Formation*	*4.61‰*	*Barrick 2010*
Australia			
Queensland	*Coral gardens Formation*	*9.02‰*	*Jeppsson et al. 2007*

It is believed that these oncoid-rich beds were formed in calm environments seaward of the reefs (Calner 2008). Beds enriched with oncoids seem to be associated with the the highest $\delta^{13}C$ values in both the Uddvide-1 (Figs. 6 and 12) and Ronehamn -1 drill core sections (Fig. 13). Small scale wrinkle structures are common in the Burgsvik Sandstone Member (Calner 2005), whereas oolite are abundant in the Burgsvik Oolite Member (Fig. 7D). The boundary between the two members is shown in Figure 7E. It is hypothesized that this microbial resurgence is related to decreased rates of grazing and infaunal activity during the event, and therefore; they can be referred to, as post-extinction ‘’disaster forms’’ (Calner 2005).

4- Material and Methods

Two core sections drilled in the south-eastern part of Gotland were described and sampled for this study (Fig. 1A). The cores have a diameter of 39 mm and were named the Ronehamn-1 core (30 m long; GPS E:1663083 N:6342406), and the Uddvide-1 core (70 m long; GPS E:1653025 N:6333020) by Eriksson and Calner (2008).

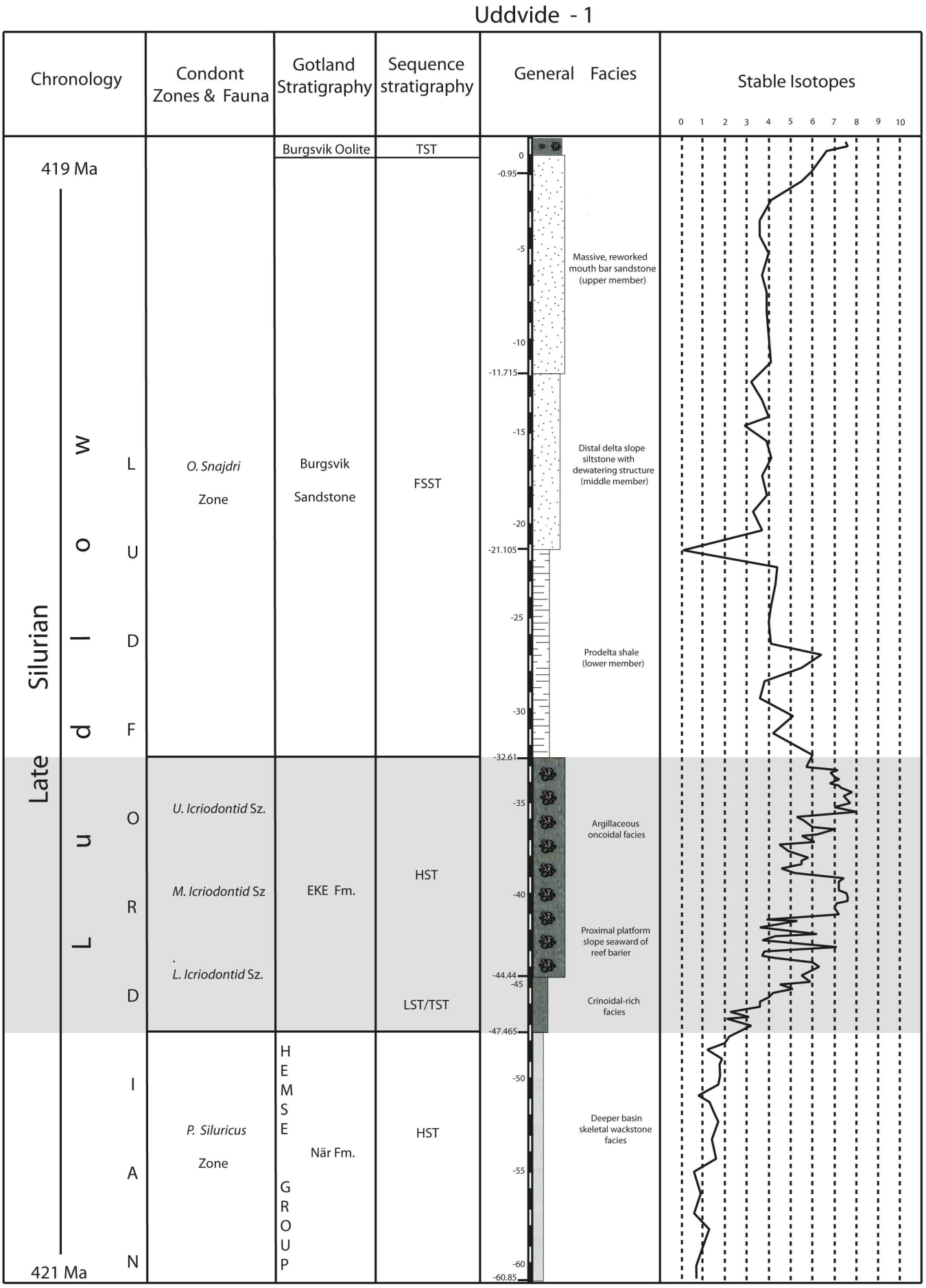

Fig. 6. Late Silurian (Ludfordian) stratigraphic framework of Gotland and carbon isotope chemostratigraphy of Uddvide-1 core. Sequence stratigraphy from Eriksson and Calner 2008. The stratigraphic range of the Lau Event is shown with light grey shading.

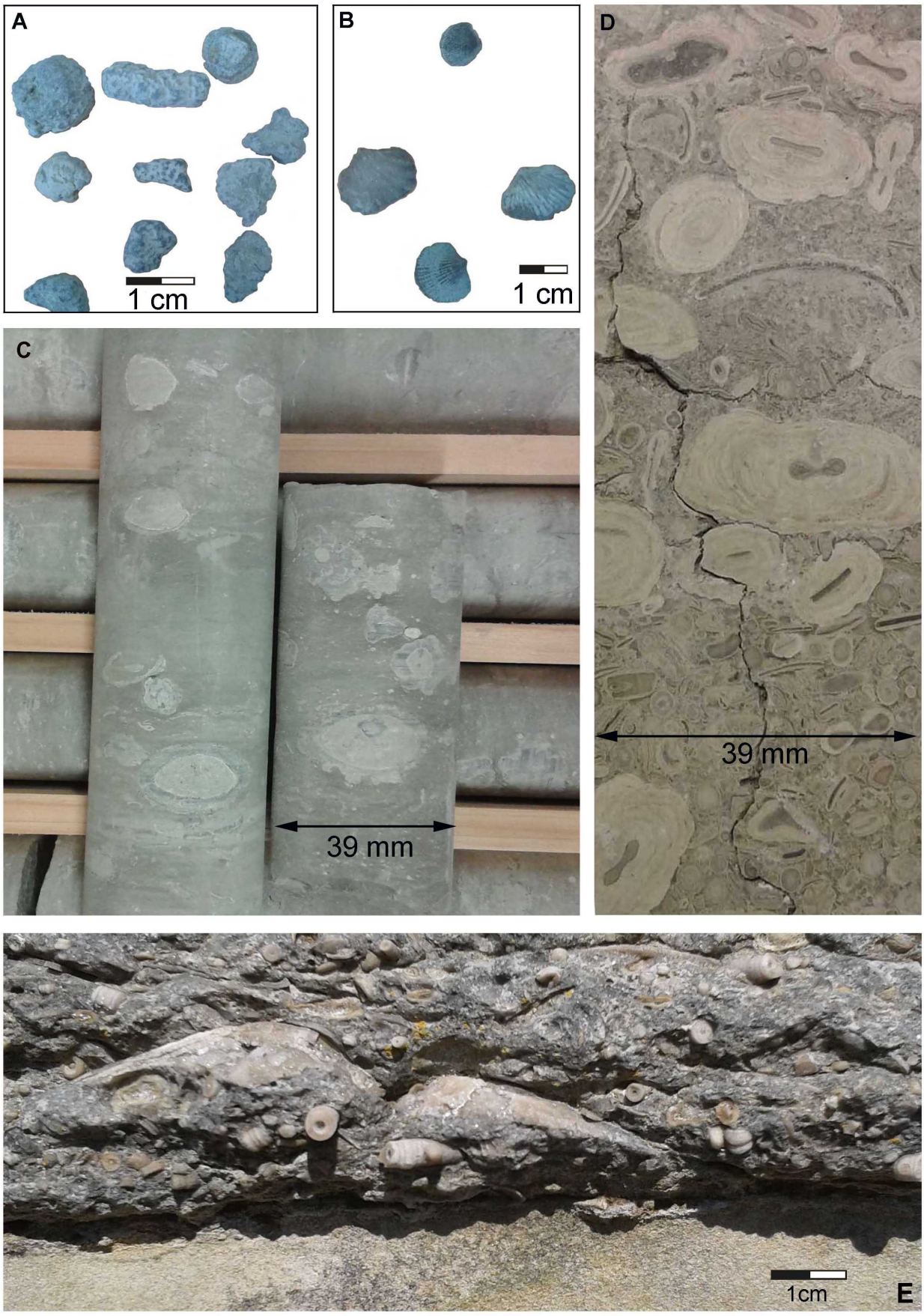

Fig. 7. Photographs showing various microbial facies related to Lau Event. **A** Oncoids obtained from Eke Formation exposed in Lau Backar-1 (locality close to the location of the Roneham-1 core, 1250 ENE of Lau Church). **B** Well preserved brachiopods from the same locality (Lau Backar.1). **C** Oncoids within the Eke formation in the Uddvide-1 core. **D** Oncoids within the Burgsvik Oolite Member in the Uddvide-1 core. **E** Image showing the boundary between the Burgsvik sandstone and Burgsvik oolite taken in SE Gotland.

The cores are stored at the Department of Geology, Lund University. Whole-rock carbon isotope samples were obtained by drilling with a microdrill and collecting the powder in small plastic cans. About 10 g of powder was recovered for each sample. In order to avoid contamination, the rugged core surface was first grinded with the core before a mm-sized hole was drilled. Skeletal grains were avoided and samples were taken from the micritic matrix of the rock. The rate of sampling was 4 sample/m in Eke formation and 2 sample/m in the adjacent formations close to both lower and upper boundaries of Eke Formation and 1 sample/m in the other parts of the core, therefore sampling intervals were less in Eke Formation (where the effect of Lau Event is detected). The samples were drilled from the two cores in the same manner. In total 77 samples of Ronehamn-1 and 118 samples of Uddvide-1 were sent to GeoZentrum Bayern in Erlangen, Germany, for analysis. The samples were subsequently reacted with 100% phosphoric acid (density >1.9; see Wachter and Hayes, 1985) at 75^{o} C using a Kiel online preparation line connected to a ThermoFinnigan 252 masspectrometer. The analyses were performed at the GeoZentrum Nordbayern of the University of Erlangen-Nuremberg, Germany. All values are reported in permil relative to the V-PDB by assigning an organic $d^{13}C$ value of +1.95‰ and an $d^{18}O$ value of -2.20% to NBS 19. Reproducibility for carbon isotope analyses was monitored by replicate analysis of laboratory standards and was better than ±0.05% (1s).

5- Results

5-1 *Sedimentary facies of the Uddvide-1 drill core*

The lithofacies occurring in the Uddvide-1 drill core are marl and limestone, clastic mudstone, siltstone and fine-grained sandstone (quartz arenite), the clastic deposits associated with the Burgsvik Formation. Based on microfacies analysis, the marl and limestone can be subdivided into the following microfacies:

Skeletal mudstone-wackestone (marl): This microfacies is common in the När Formation, which occupies the lowermost 13-14 m of the Uddvide-1 drill core. This formation consists mainly of aggrading limestone-marl alternations with some finely laminated beds (Fig. 8A), suggesting low rates of infaunal activity and a slightly dysoxic depositional setting. The presence of graptolite fragments suggests a deeper carbonate platform depositional environment.

Crinoidal packstone-wackstone: Unlike the När Formation, abundant crinoidal derbis at the base of Eke Formation indicates normal marine subtidal conditions; this aggraditional zone comprises wackestone-packstone facies, limestone interbeds, stromatolite fragments and abundance of whitish grains of crinoids (Fig. 8B). They are together indicating shallower depositional setting as compared to the underlying När Formation. The thickness of the crinoidal-rich unit, which also includes fragments of trilobites and brachiopods, is almost 3 m. The Botvide Member is absent due to erosion and is directly deposited at the conformable boundary between Eke and När formation (Fig. 8C) (Calner 2008).

Oncoidal packstone: A progradational oncoidal packstone facies represents most of the Eke Formation (except the lower crinoidal zone). It is about 14 m thick in the Uddvide-1 drill core. It comprises wackestone-packstone with an argillaceous matrix rich in silt-sized quartz and a fossil content similar to the crinoidal-rich unit, in addition to high abundance of oncoids (Calner 2008). The oncoids are bluish-grey coloured and have diameters varying from few millimetres up to ca 3-4 cm. Their shape varies from spherical with cement infilling in the nuclei to non-spherical, irregularly formed shells. The cortex varies in thickness from a few millimetres to more than 10 millimetres and is almost in the thicker end of that range (Fig. 8D). In addition to oncoids, a few shell fragments of graptolites, brachiopods, and corals were identified. Siliclastic strata: The siliciclastic strata are confined to the Burgsvik Sandstone Member of the Burgsvik Formation. These strata are ca. 32.5 metre thick (Calner 2008). The lowermost part of this member comprises barren prodelta shale with rare, thin interbeds of siltstone (Fig. 9A). The middle part comprises siltstone and almost planar laminated interbeds of fine-grained sandstone, the dewatering structures preserved in siliclastic rocks can be easily observed (Fig. 9B). The upper member consists of massive, fine-grained sandstone (Fig. 9C). The Burgsvik Sandstone Member is unconformably overlain by the Burgsvik Oolite Member, which constitute oolite grainstone and oncoidal rudstone (Fig. 9D).

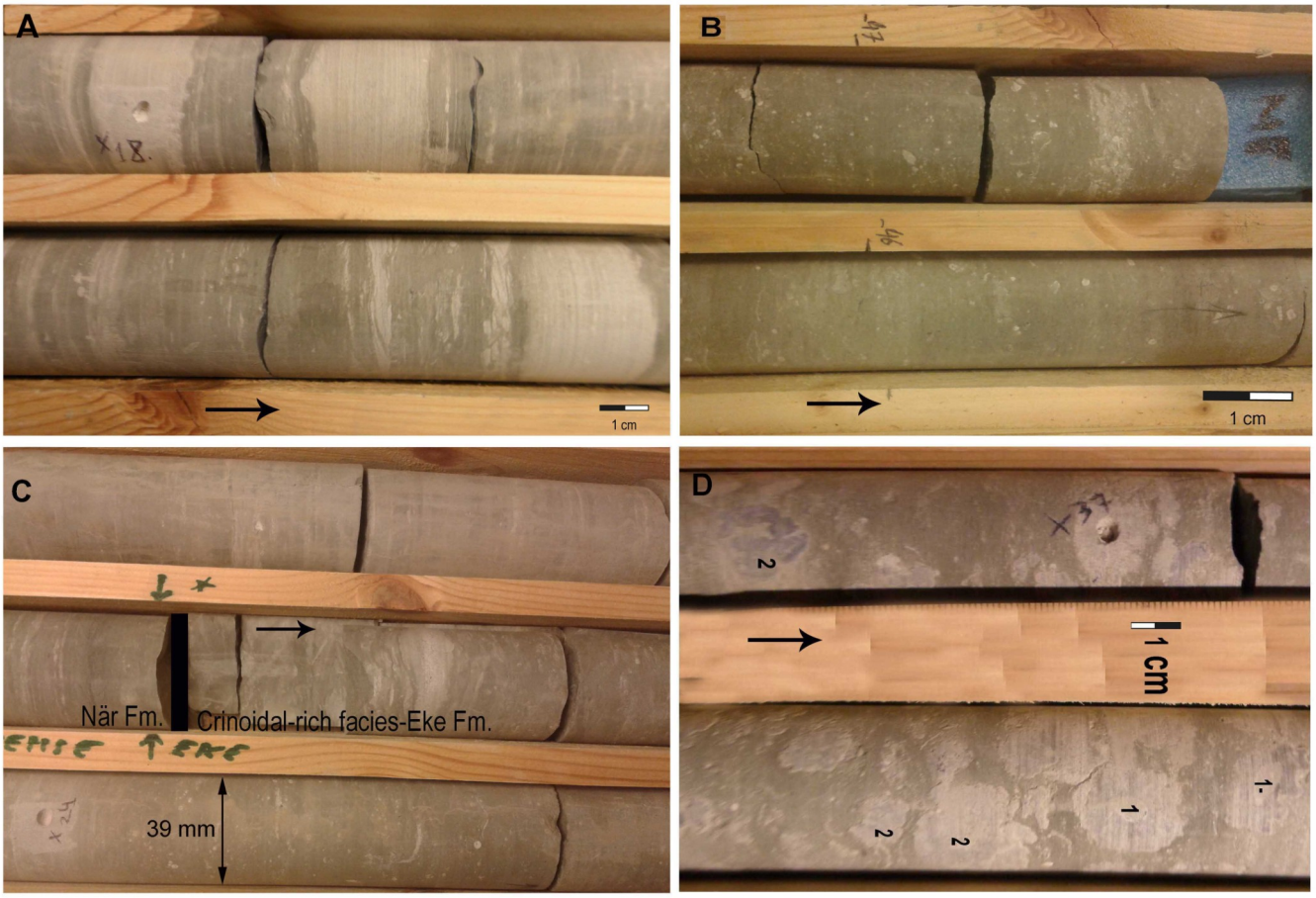

Fig. 8. Photographs showing facies characteristics of the Uddvide-1 core section. **A** Limestone-marl alteration of the När Formation. **B** Crinoid fragments within crinoids-rich zone of the Eke Formation. **C** The boundary between the När Formation and the crinoidal-rich zone of the basal Eke Formation. **D** A part from Eke Formation containing oncoids and showing 1 nucleaus and 2 cortex.

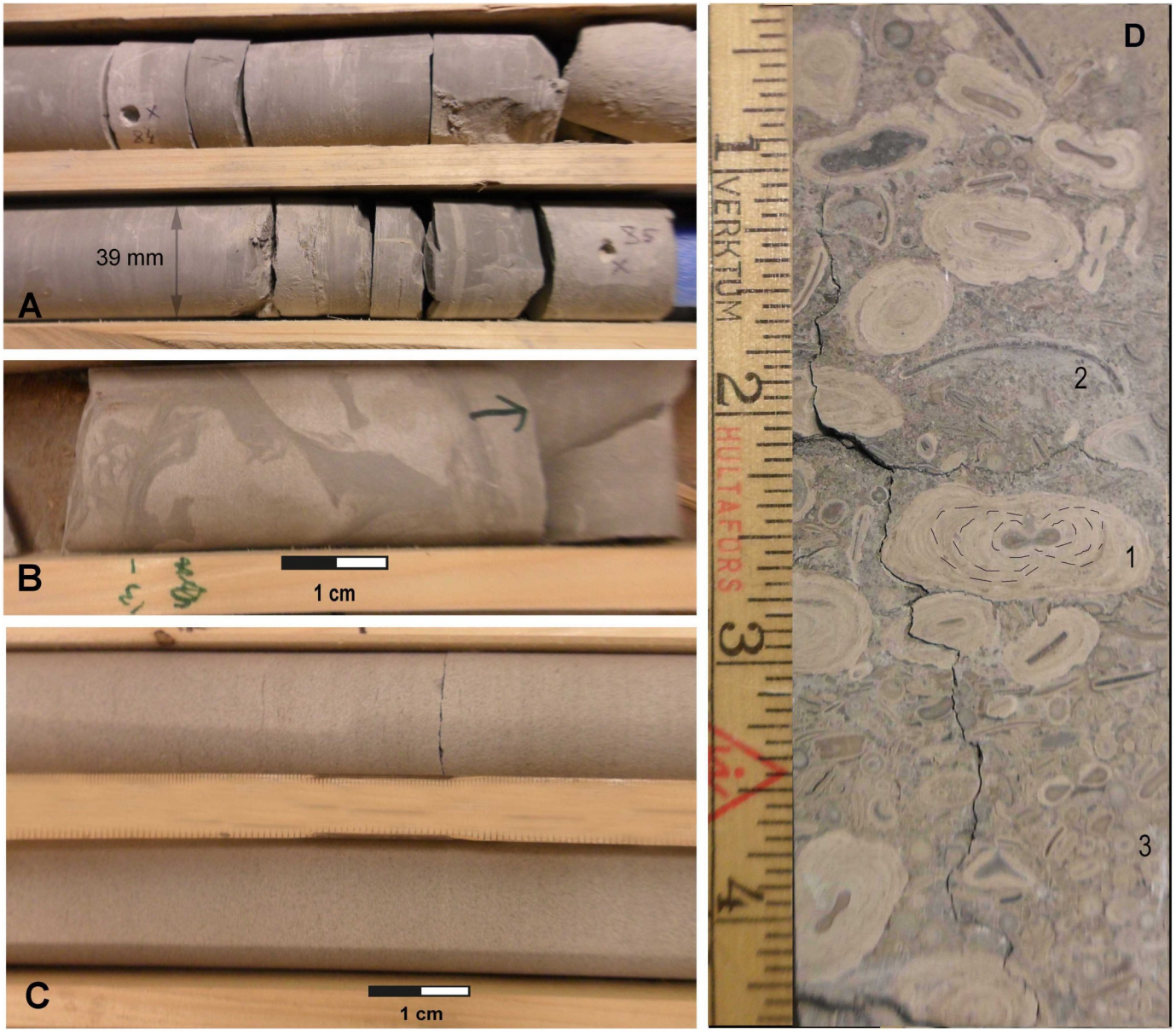

Fig. 9. Photographs showing facies characteristics of the Burgsvik Formation in the Uddvide-1 drill core. **A** Prodelta shale of the lower informal member of the Burgsvik sandstone. **B** Siltstone with dewatering structures of the middle informal member of the Burgsvik sandstone. **C** Massive sandstone bar of the upper informal member in Burgsvik sandstone. **D** Photograph of the Burgsvik Oolite showing 1 spherical oncoid with cement infilling in the nuclei and 2 non-spherical, irregularly formed shells, and 3 ooids.

5-2 *Sedimentary facies of the Ronehamn-1drill core*

The lithofacies occurring in the Ronehamn-1 drill core are very similar to those of Uddvide-1. The only difference is that -unlike Uddvide-1- Botvide Member is preserved in Ronehamn-1 and that only the basal part of the siliciclastic strata are preserved in Ronehamn-1 (due to post-Silurian erosion). The following microfacies are identified:

Skeletal mudstone-wackestone (marl): represented by the När Formation which occupies the lowermost ca. 13.5 m of the drill core section. The formation comprises massive mudstone-wackestone with trace fossils (*Chondrites*), and includes thin interbedded limestone layers (Fig. 11A). Skeletal fragments of brachiopods and other faunal contents are obviously seen in this layer (Fig. 11C). The faunal content including mainly conodonts, graptolites and trilobites is more diverse in Ronehamn-1 than in Uddvide-1 suggesting a more shallow environment seaward of the reef barrier.

The uppermost centimetres of the När Formation (below Botvide Member) comprises flat-pebble conglomerates indicating relative shallowing (cf. Myrow et al 2004). The Botvide Member (the uppermost ca 1 m of the När Formation) comprises intraclastic skeletal packstone and grainstone (Fig. 11B), and displays an upper minor erosional boundary towards the Eke Formation.

Crinoidal wackestone-packstone: This unit is almost 1 m thick at the base of Eke Formation. The unit is characterized by the abundance of crinoid fragments, limestone interbeds in addition to some other faunal fragments (stromatolites, brachiopods, trilobites). The base of this zone includes a flat-pebble conglomerate.

Oncoidal wackestone-packstone: this progradational facies comprises most of the Eke Formation (except the crinoidal zone) and is ca 11 m thick. The fossil contents of particularly oncoids (Fig. 10), corals and brachiopods increase upwards through this unit. Also the microfacies get coarser and change from wackestone in the lower part to packstone in the upper part. The oncoids (Fig. 11D) have diameters varying from a few millimetres up to 4-5 centimetres; their increasing abundance in upper levels of Eke Formation reflects a shallowing -upwards environment with successively increasing water energy.

Siliclastic strata: In the Ronehamn-1 core only the lowermost two meters of Burgsvik Formation is preserved. The strata consist of ca. 1.5 m thick argillaceous facies and ca. 0.5 m of siltstone.

Fig. 10. Photograph showing oncoids within Eke Formation in in Ronehamn-1 drill core.

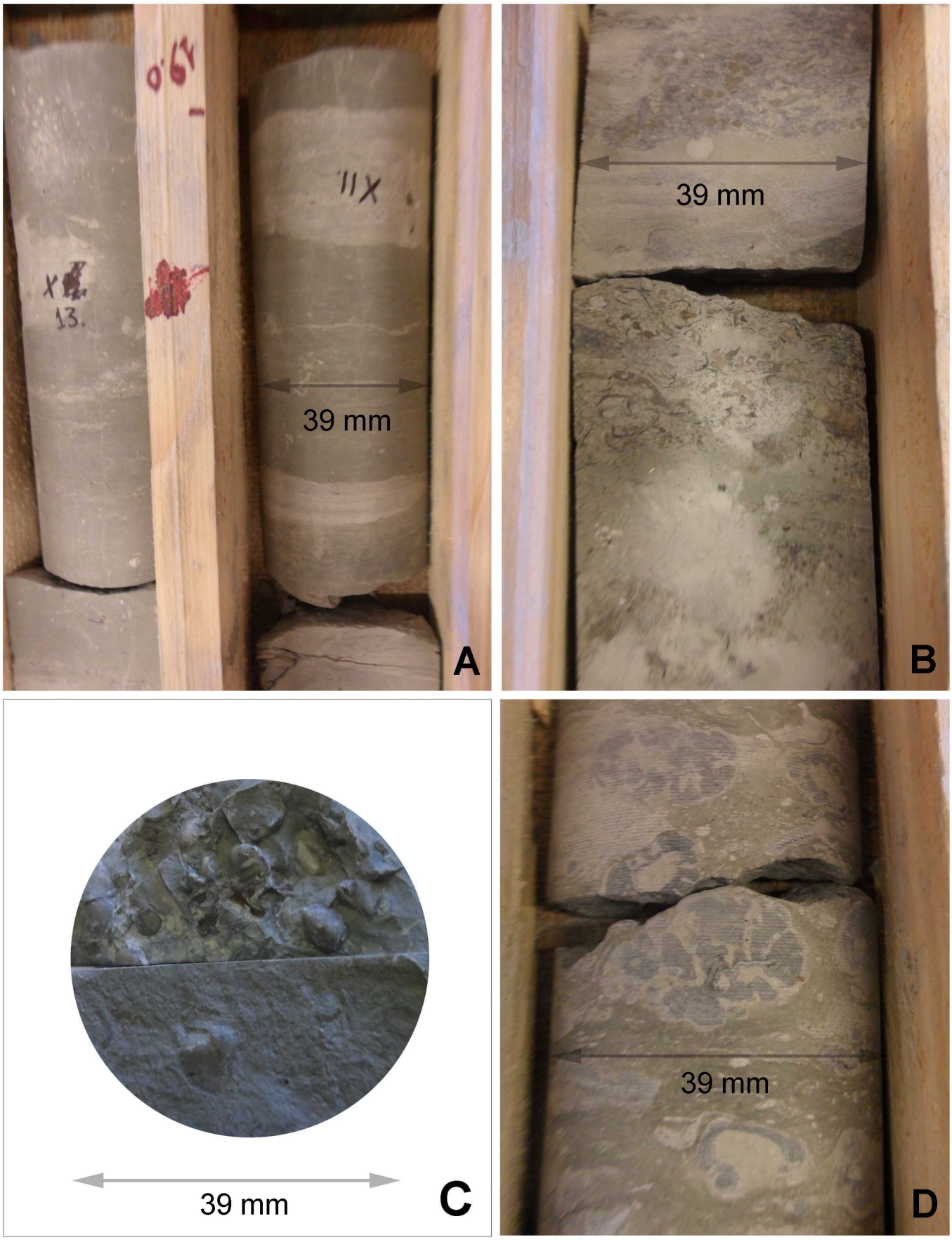

Fig. 11. Photographs showing facies characteristics of Ronehamn-1 drill core. **A** Marl with limestone interbeds within När Formation. **B** Botvide Member. **C** Skeletal fragments of brachiopods within När Formation. **D** Oncoids fragments within Eke Formation.

5-3 *Carbon isotope chemo-stratigraphy*

In both of the studied core sections, Uddvide-1 and Ronehamn-1, a strong positive shift in $\delta^{13}C$ values is observed in the sediments covering the Lau Event interval (Figs. 6, 12 and 13). In Uddvide-1: $\delta^{13}C$ values are about 0.62 ‰ to 1.85 ‰ through most of the upper part of the När Formation and they increase to 2.35‰ in its uppermost part, just before the boundary with the Eke Formation (Table 2 in Appendix A; Figs. 6, 12). $\delta^{13}C$ values continue to gradually rise through the lowermost 2.25 m of the Eke Formation (crinoidal-rich zone), from 3.22 ‰ at the base of the crinoidal zone, to as high as 5.10 ‰ near the top of that zone. Values are fluctuating through the Eke Formation, with a tendency to rise, but generally forming a plateau that corresponds in time with the oncoid-rich part of the Eke Formation, and attain peak values between 7.21 ‰ and 8.03 ‰ in the upper part of Eke Formation before the declining limb of carbon isotope excursion starts. A single taxon (Icriodontid) dominated the conodont fauna during the time interval corresponding to the plateau. The $\delta^{13}C$ values fall at the boundary between Eke Formation and Burgsvik Formation (Figs. 6, 12 and Table 2). It is notable that high $\delta^{13}C$ values are re-established in the Burgsvik Oolite Member similar to those of the plateau that prevailed during the event (Table 2). This may be related to the existence of microbial fossils in the Burgsvik Oolite Member, which also includes abundant oncoids (Fig. 12). By linking the rapid stepwise extinctions to the $\delta^{13}C$ chemostratigraphy of the Uddvide-1 drill core (Fig. 5 and Table 2), it is shown that the extinction was accompanied with gradually increasing $\delta^{13}C$ values. The average $\delta^{13}C$ values after the falling limb, i.e. In the Burgsvik Sandstone Member, is still relative- ly high and much higher than the $\delta^{13}C$ base line values before the initial rising limb (Fig. 12). This can be interpreted as due to the disappearance of oncoids or because the isotope values reflect the diagenetic cement in the sandstone rather than skeletal grains and micritic matrix as in the other samples. If so, the slight drop in $\delta^{13}C$ values is due to sedimentary facies change rather than to the end of The Lau Event. The renewed rise in $\delta^{13}C$ values in the Burgsvik Oolite Member can support this interpretation (Fig. 12). The similarity in correlation with COG section (mentioned later in this study) can provide additional support to this assumption. In the Ronehamn-1 drill core, the average value of $\delta^{13}C$ through the När Formation (except Botvide Member) is 1.28 ‰. The values steeply rise through Botvide Member (the uppermost 0.87 m of the När Formation) from 1.83 ‰ to 5.06 ‰. $\delta^{13}C$ values fluctuate through Eke Formation and they have general tendency to rise gradually from averagely 5.17 ‰ through the lowermost 1.01 m of the Eke Formation (crinoidal-rich zone). They attain peak values between 8.58 ‰ and 9.01 ‰ in the uppermost part of the Eke Formation before they start declining in Burgsvik Formation (Table 3 in Appendix B; Fig. 13).

It is clear in that the low-diversity Icriodontid Zone coincides with a plateau in the $\delta^{13}C$ curve, and the highest values of $\delta^{13}C$ coincide with the Upper Icriodontid conodont subzone (Fig. 5).

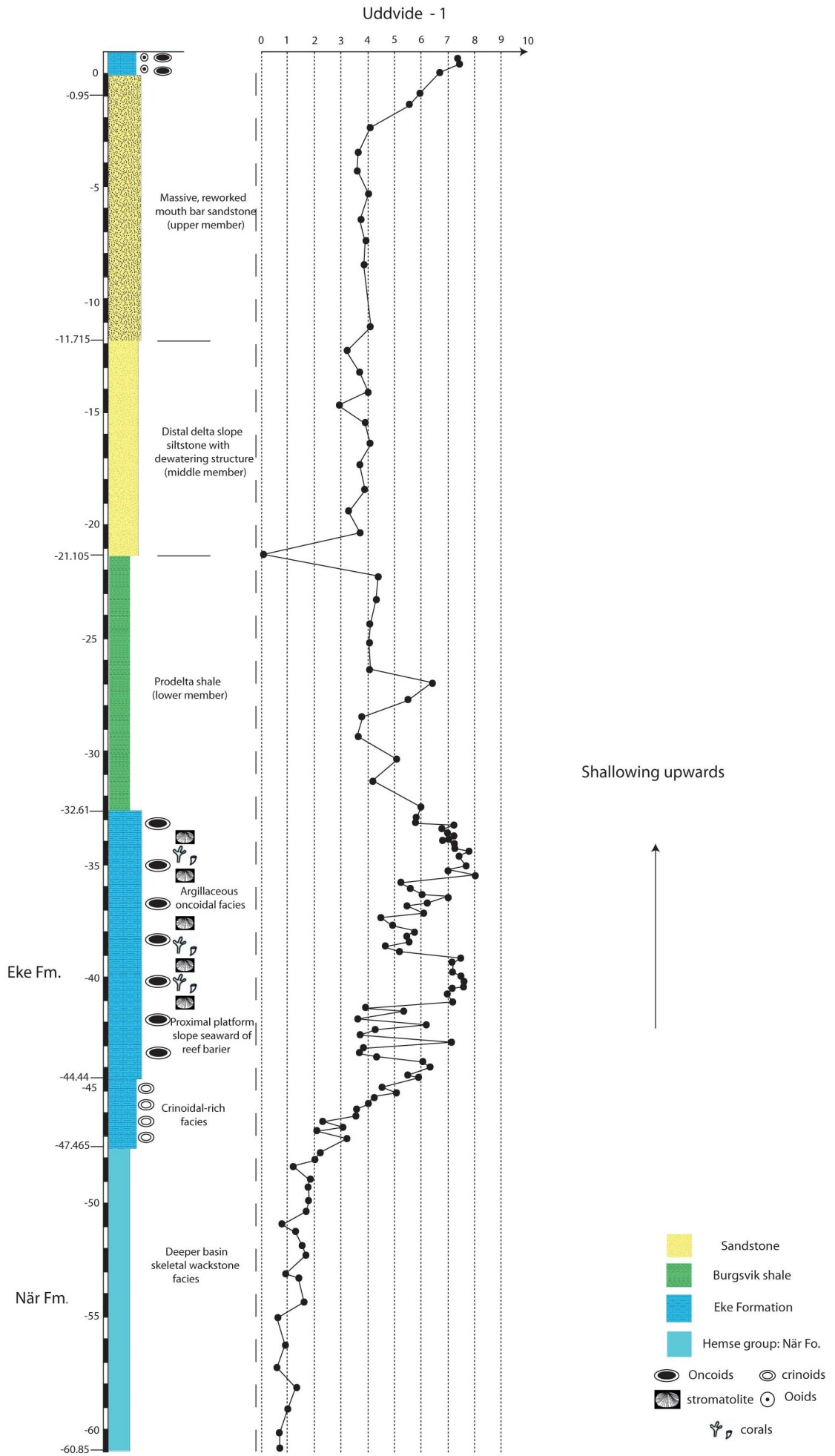

Fig. 12. Illustration showing The Uddvide-1 core section and the established $\delta^{13}C$ stratigraphy.

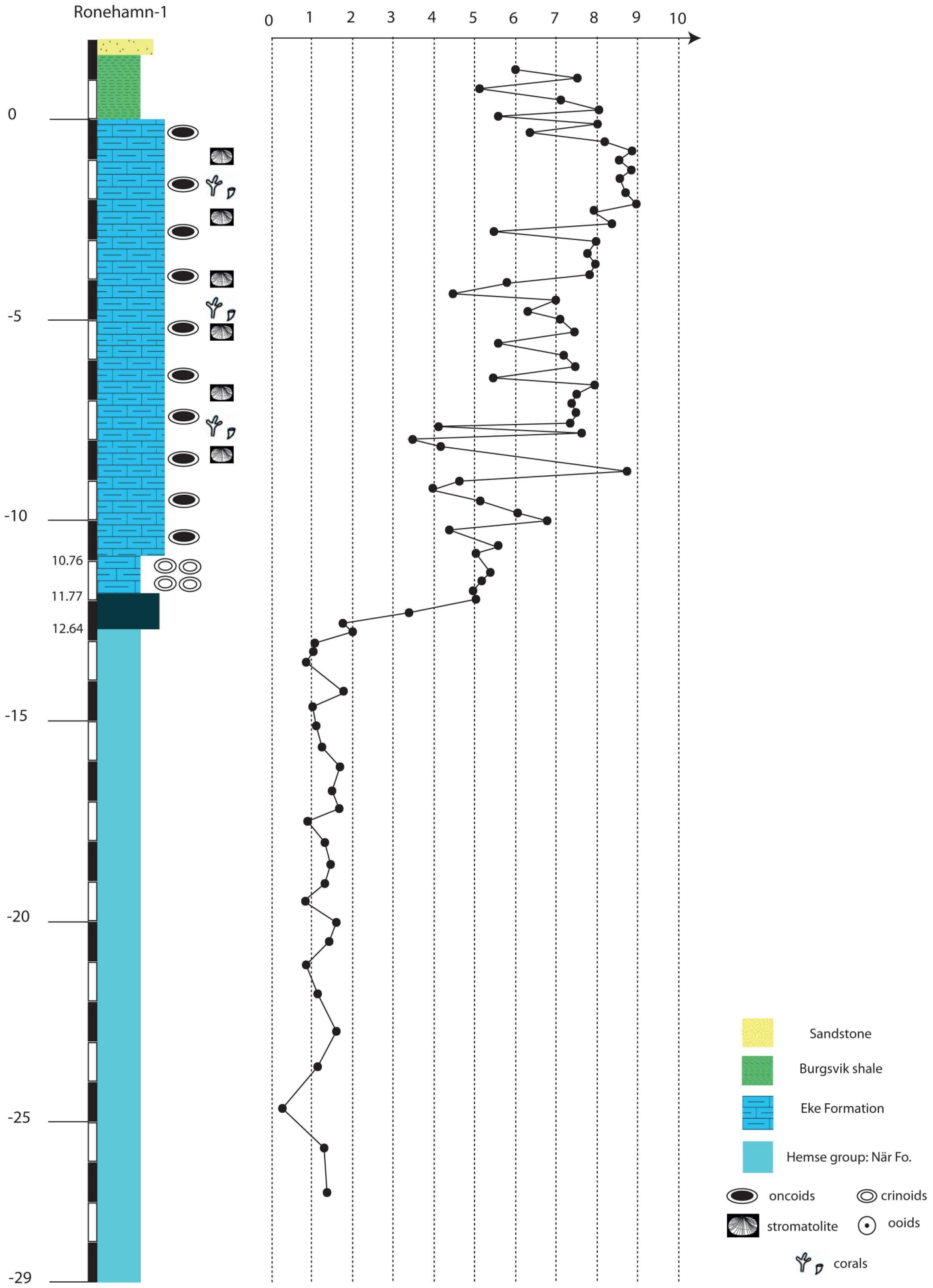

Fig. 13. Illustration showing The Ronehamn-1 core section and the established $\delta^{13}C$ stratigraphy .

6- Discussion

It is well known that the environmental changes in marine ecosystems correlate with changes in isotopic ratios of some elements in atmospheric gases, animals and plant tissues, the carbonates of teeth, corals, soils and the organic matter deposited in sediments. Carbon is considered one of those chemical elements, and it is the most effective proxy for environmental changes. Most biotic events in Earth history are associated with anomalies in the $^{13}C/^{12}C$ ratio and carbon isotope chemostratigraphy therefore plays an important role in the study of mass extinctions as well as minor biotic turnovers. The method provides us with valuable information about the synchronicity of environmental changes on local, regional and global levels (Coleman and Fry 1991). Carbon isotope chemostratigraphy utilises minor changes in the ratios of $^{13}C/^{12}C$ (the relative abundance of ^{13}C and ^{12}C in nature is ≈ 1:99), which are reported relative to an international standard using a delta notation; $\delta^{13}C = (^{13}C/^{12}C\ -1)*1000$ (Todd E. Dawson and Rolf T.W. Seigwolf 2007). Valuable information about both processes and sources could be calculated from the ratio of rare-to-common (or heavy to lighter) stable isotope of a particular element like the ratio $^{13}C/^{12}C$. Since the World oceans contain about 50 times as much carbon as the atmosphere, the oceanic carbon cycle is considered the main sink determining the large perturbations in atmospheric CO_2 during interglacial and glacial cycles (Bopp and Le Quèrè 2009). Carbon sequestered in marine organisms throughout geological time controls to a large extent the geochemical disequilibrium of our planet. Biological sequestration of carbon in the ocean– controlled by nutrient export flux is the main factor controlling the changes in atmospheric CO_2 during interglacial-glacial transitions (Longhurst 1991). The sudden rise in carbon isotope values at the beginning of a carbon isotope excursion is considered to be a marker for the onset of changes in oceanic carbon cycle (Brenchley et al. 2003). The biologically-mediated processes that transport carbon from the ocean surface waters to the deep layers of ocean waters are referred to as the ‘’biological pump’’ (Longhurst 1991). Whereas the surface layer of the ocean is in equilibrium with the atmosphere, the deeper water layers are oversaturated with dissolved CO_2, the gravitational settling of organic carbonate C fixed by plant cells in surface water maintain the sinking flux of C (Longhurst 1991). Since carbon flux is produced in surface water, it is very important to take into account the properties of these surface water layers like salinity, nutrient abundance and the thickness of the photosynthesis zone. High productivity resulting from high nutrient supply occurred during the time of sea-level lowstand (Botvide Member and Lower Eke Formation) and was interpreted as the reason of Late Silurian $\delta^{13}C$ excursion on Gotland by Wenzel & Joachimski (1996).

6-1 *A chemostratigraphic model for the Lau Event*

As documented from several parts of the World, the morphology of the Lau Event $\delta^{13}C$ profile includes a relatively short, gradually rising limb followed by a plateau with constant or slightly rising values, and then a gradually falling limb (Kaljo et al. 2007; Jeppsson et al. 2007 and Barrick 2010). The $\delta^{13}C$ profile documented herein from the Uddvide-1 drill core is thus representative for the

Lau Event as recognised in other palaeocontinents. The rising limb can be steep, such as in the Ronehamn-1 drill core, where it coincides with a minor unconformity located at the boundary between the Botvide Member and the Eke Formation (Figs. 6, 12 and 13). The carbon isotope curves from the Uddvide-1 and Ronehamn-1 cores show a very similar development. Since only the Uddvide-1 core, however, shows a complete record for the entire event, i.e. including also the Burgsvik Formation, this discussion will be focused on this curve. The similar relationship between the chemostratigraphy and biostratigraphy throughout the Baltic region (Gotland Sweden, Holy Cross Mountains Poland, and East Baltica) suggest that it has a regional chemostratigraphic value. Also, the similarity in shape as well -in most cases- and in magnitude of the carbon isotope excursions indicate that this is a global excursion that can be used for detailed chemostratigraphic correlation on intercontinental basis. Here, I describe the morphology and characteristics of carbon isotope excursion of the Lau Event and correlate positive excursions detected on different palaeocontinents in the same way as Brenchley et al. (2003) did for the Late Ordovician mass extinction. Five stratigraphic levels (datums) of conodont extinctions were identified for the Lau Event by Jeppsson et al. (1993). The Lau Event encompasses two oceanic cycles, namely one Primo and one Secundo episode. Key levels of environmental changes have been identified along the carbon isotope profile. Low, stable, and slowly increasing $\delta^{13}C$ values are associated with the Primo Episode, whereas initially high, slowly decreasing values are associated with the Lau Event and the initial part of the succeeding Secundo Episode (Talent et al., 1993; Samtleben et al. 1996, 2000; Wenzel and Joachimski 1996; Wenzel 1997; Saltzman 2001; Cramer and Saltzman 2005). Figure 14 overviews the chemostratigraphical model with sea level changes. The $\delta^{13}C$ curve forms a base line of low or even negative values shortly before the event starts: +1 on Gotland (this study) and in Bohemia (Lehnert 2007), -1 in Podolia, Ukraine (Kaljo et al. 2007), and + 0.5 in both Australia (Jeppsson et al. 2007) and USA (Barrick 2010). The rising limb correlates with the onset of the extinction, before a plateau is established, and corresponds in time with the lowermost Eke Formation in Gotland, the Winnica Formation in Poland and the Coral Gardens Formation in Queensland, Australia. The plateau displays stable values that scatter around 6.5 ‰ in the Uddvide-1 core and 7.5 ‰ in the Ronehamn-1 core on Gotland (this study), 4 ‰ in Podolia Ukraine, and 5 ‰ in Southern Laurentia. The plateau is coeval with a high-stand systems tract (HST) on Gotland and coincides with the most impoverished conodont and graptolite faunas (Fig. 14). The absence of a plateau in some curves most likely results from weathering and erosion of the corresponding strata. Some other differences in the compiled curves can result from meteoric digenesis, by mistakes in sampling, or by laboratory treatment. The decreasing of $\delta^{13}C$ values within the Burgsvik Sandstone Member, where we have moderate faunal diversity, can be interpreted either as the re-appearance of predators of microbial organisms or by sedimentary facies change. The increasing of $\delta^{13}C$ values again in Burgsvik Oolite Member supports the second hypothesis (Fig. 12).

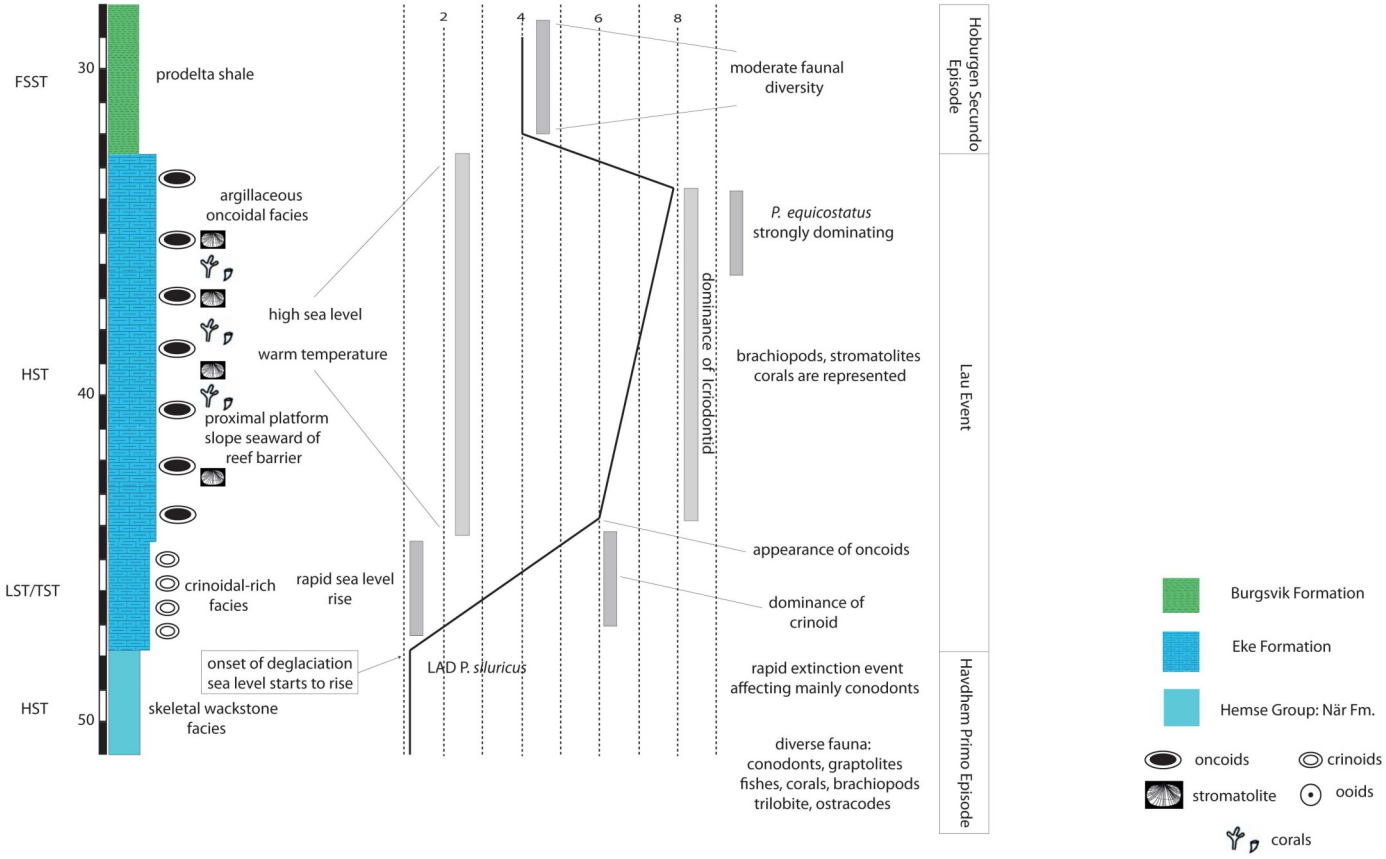

Fig. 14. Summary diagram showing the stratigraphy and evolution of the Lau Event carbon isotope curve.

6-2 *Chemostratigraphical correlations*

In case of rapid environmental change, correlation based on chemostratigraphy is of a higher resolution than that based on biostratigraphy (Brenchley et al. 2003). Consequently, chemostratigraphical correlation is very useful in studying the similarities and differences in the patterns of the Lau Event on different palaeocontinents (see Fig. 15 in Appendix A). Here $\delta^{13}C$ profiles from different palaeocontinents are compared to the $\delta^{13}C$ profile of the Uddvide-1 drill core.

Long-term sea-level changes are caused by either climatic processes or by plate tectonics (Coe and Church 2003). Plate tectonics control sea-level change by modifying the size and shape of ocean basins (Coe and Church 2003). Metamorphism and strong tectonic processes are not evident in the strata of Gotland (Jeppsson 2005). As such, with regard to this study, climatic processes are considered alone to be the cause of sea-level change (Eriksson and Calner 2008). Climatic processes control sea-level change either through the formation or melting of ice-caps and glaciers, or through the thermal expansion of oceans (Coe and Church 2003). Changes in the oceanic carbon cycle effect changes in carbon isotope values and are linked to the onset of glaciation and sea level change (Brenchley 2003). Substantial base-level changes during the Lau Event played an important role in sedimentary changes, such as the development of discontinuity surfaces, microbial faunal activity (*Rothplezella* and *Wetherdella*), the influx of sediments into the basin, and the widespread distribution of intraclastic and flat-pebble conglumerates. Some models for Lau Event of Gotland suggest that two regressions coincide with two glaciation periods; the first corresponds to the palaeo-karst associated with the crinoidal-rich facies in the Lower Eke Formation, and the second one with the Burgsvik sandstone facies (Eriksson and Calner 2008).

6-2-1 *Uddvide-1, Gotland vs COG, north-eastern Australia*

The studied area in north-eastern Australia was located on the eastern margin of Gondwana during the Late Silurian (Cocks and Torsvik 2002), while Gotland was formed within the Baltic Basin during the same epoch (Barrli et al. 2003). Facies with corresponding isotopic ratios of both the Uddvide-1 and COG sections are shown in Figure 16. The length of the Uddvide-1 drill core from its base to approximately 47.5 m is comprised of the Upper Hemse Group. The $\delta^{13}C$ values obtained from this length show a slight increase with an average baseline of around 1.5‰. The length of the COG section from approximately 14 m to 43.5 m encompasses the argillite and limestone beds of the Coral Gardens Formation, a length equivalent to the Upper Hemse Group in the Uddvide-1 drill core. The $\delta^{13}C$ values of this length show a similar increase with an average base line of around 1‰. The $\delta^{13}C$ values of both lengths are similar, ranging from around 0.5‰ to 1.5‰ before reaching their highest value at the boundary with the overlying formation/ sub-formation. The $\delta^{13}C$ values of the rising limb in the COG section, which corresponds with dark flaggy bioclastic micrites, increase suddenly from around 2‰ to more than 6‰. The $\delta^{13}C$ values of the rising limb in the Uddvide-1 core section, which corresponds with the crinoidal-rich facies of

the lowermost 3 meters of the Eke Formation, increase gradually from 1.5‰ to 6‰. The difference between the rising limbs of the two sections can be explained by the presence of the carbonate-rich dark flaggy bioclastic micrites in the COG section (Jeppsson et al. 2007). The equivalent carbonate-rich layer (the Botvide Member) is not present in the Uddvide-1 core section (Eriksson and Calner 2008). The onset of the CIE corresponds with the onset of forced regression in both COG and Uddvide-1 sections. They continued to increase within the latter system tracts. The $\delta^{13}C$ values of the oncoidal-rich Eke Formation form a plateau with a slightly rising trend fluctuating between 6‰ to 8‰. The thickness of this part is around 12 m. The coeval $\delta^{13}C$ profile in the COG section shows the same morphology forming a similar plateau to that of Uddvide-1, with slightly rising values scattering between 6‰ and 7‰. It is difficult to decide If the gradually decreasing $\delta^{13}C$ values in the Burgsvik Sandstone Member are because of changes in sedimentary facies linked to the falling sea level or because of different diagenesis or some other reason. Since faunal fossils with carbonate shells are near absent in the Bursgsvik Sandstone Member, the relatively high $\delta^{13}C$ values through this member could be interpreted as non-organic ^{13}C stable isotopes sequestered in cement. The equivalent part of COG section shows the same isotopic and facies changes as shown in Figure 16. $\delta^{13}C$ values rise again in oolitic sandstone layers in both sections.

6-2-2 *Uddvide-1, Gotland vs Baltica*

The correlated cores in this passage are located on the same palaeocontinent (Baltica) and their facies and isotopic ratios are shown in Fig. 17.

Data used in the correlation is obtained from Kaljo et al. (2007) for correlation with Zhvanets 39 from Podolia, Ukrain, and from Kozlowski and Munnecke (2012) for correlation with the Rzepin section, Holy Cross Mountains (HCM), Poland.

The $\delta^{13}C$ profiles from the shared parts of the Uddvide-1 and Ronehamn-1 core sections are very similar, ranging between 0.5‰ and 1.5‰ before they reach a value of 2‰ at the onset of the rising limb. The $\delta^{13}C$ values started to rise at the boundary between Eke and När Formations, whereas they started to rise at the base of Botvide Member reflecting lateral facies changes (Fig. 17). The rising limb shows a steep trend in Ronehamn-1 corresponding to the Botvide Member which is absent in Uddvide-1 core. The Botvide Member forms the uppermost part of Hemse Group and is terminated upwards by a minor erosional hardground surface, whereas the boundary between the När and Eke formations is conformable in the Uddvide-1 core section (Calner 2008). The $\delta^{13}C$ profile from the Zhvanets 39 section has average base line values of about 0‰ before the onset of positive excursion at the boundary towards the overlying Grinchuk subformation. $\delta^{13}C$ values start to increase gradually at the very bottom of the Isakovtsy dolomites subformation in similar way to Uddvide-1 with initial value of 1.3‰ and increase steadily to more than 4‰ at the end of the rising limb. The onset of the $\delta^{13}C$ positive excursion in Zhvanets 39 is coeval with the change in sedimentary facies at the boundary between Grinchuk and Iskovtsy subformations. Data of $\delta^{13}C$ rising limb values are missing in Rzepin section, Poland.

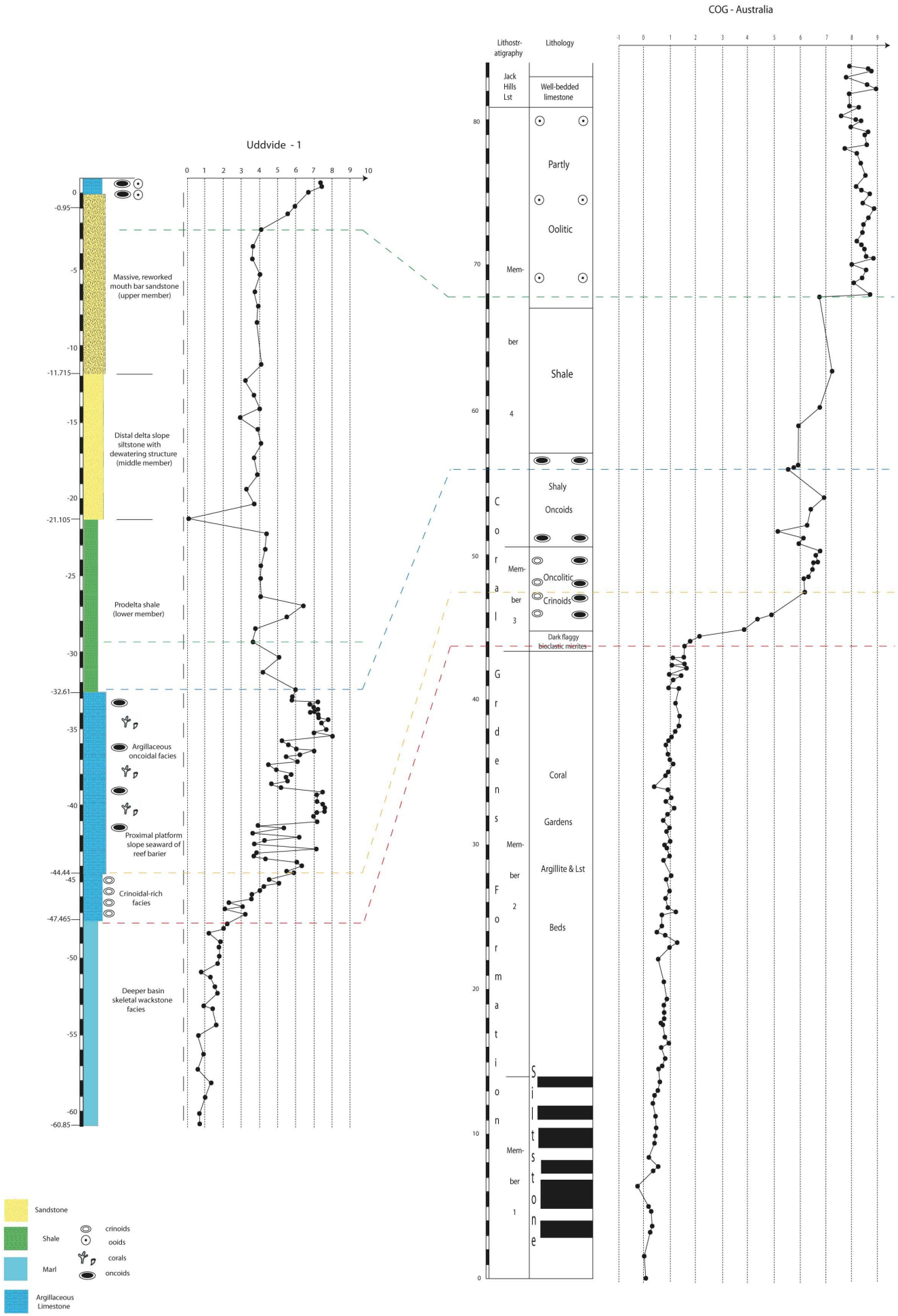

Fig. 16. Chemostratigraphical correlation of the Lau Event between Uddvide-1, Gotland and COG, North-East Australia.

The $\delta^{13}C$ profiles from all sections have similar slightly rising plateau reaching a peak of 8.03‰ in Uddvide-1, 9.01‰ in Ronehamn-1, 6.6‰ in Zhvanets 39, and 8.9‰ in the Rzepin section. The thickness of the corresponding strata (of the plateau) is obviously very different between different sections. This variation is in turn related to varying depositional settings and linked to sea level change (different sedimentation rate). This can be interpreted due to the studied sections are located in different areas with different local tectonic regimes. For example, the HCM where we have the longest $\delta^{13}C$ plateau and thus highest net depositional rates, is located in the fordeep of a foreland basin, while sediments of Gotland (which are thinner than the HCM sediments) have been deposited in the cratonic interiors of the same foreland basin (Kozlowski and Munnecke 2012). It is known that the sediments of east Baltica have been deposited in a shallower water environment than those of Gotland. Whilst the falling limb is missing in Ronehamn-1 and is incomplete in Zhvanets 39, with a decreasing rate of ca 1 ‰ per m, it shows the same trend in Rzepin and Uddvide-1 sections. falling limbs in both of them show gradual decreasing from ≈ 6‰ to base line of ≈ 1‰ in Rzepin and from ≈ 6‰ to base line of ≈ 4‰ in Uddvide-1.

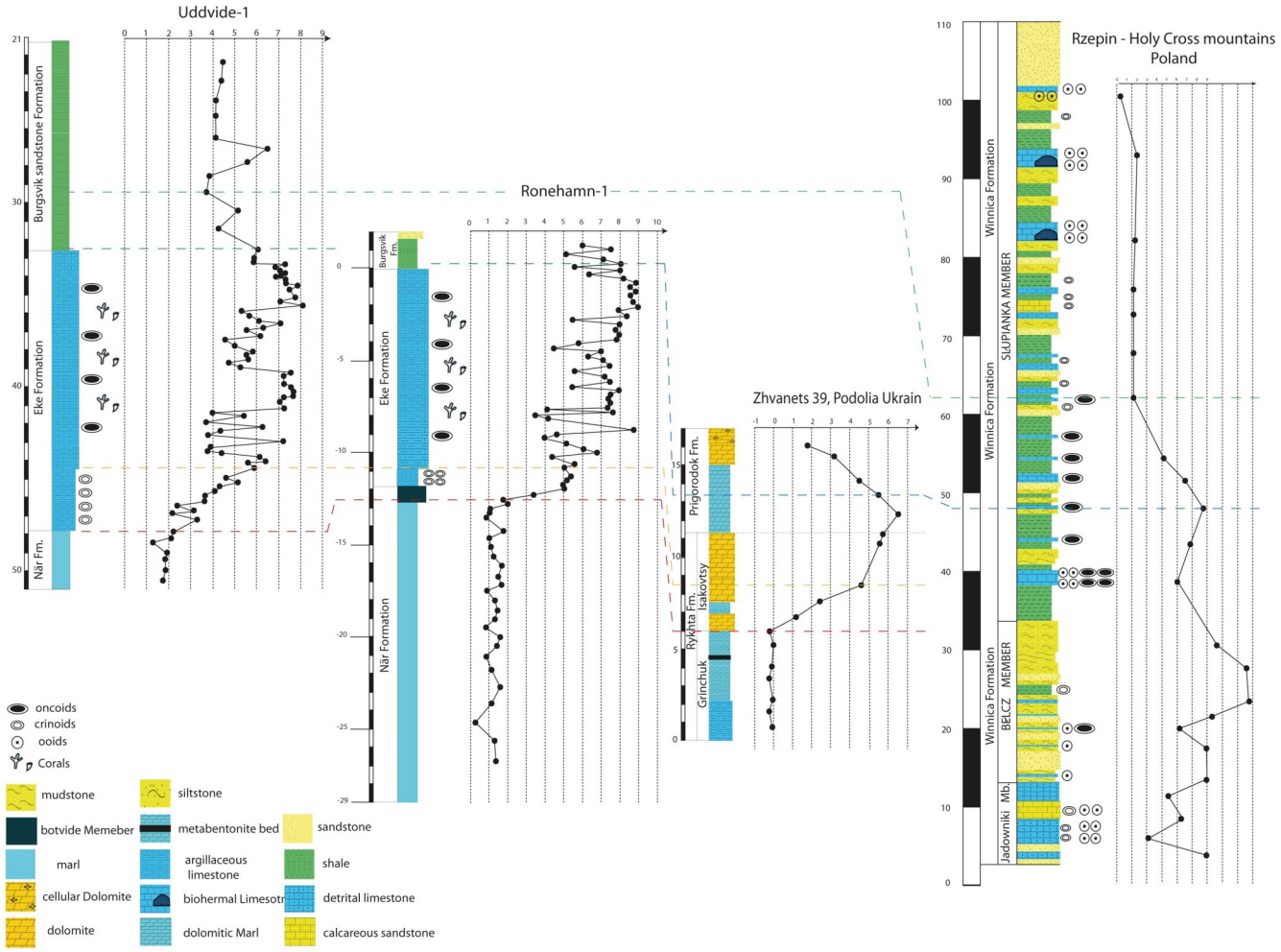

Fig. 17. Chemostratigraphical correlation of the Lau Event on Baltica.

6-2-3 *Uddvide-1, Gotland vs Bohemia*

Unlike Baltica, which was located within tropical and subtropical latitudes, the Prague Basin was located in middle southern latitudes of northern Peri-Gondwana during the Late Silurian (Lehnert et al. 2007). Isotopic data used in this correlation is obtained from Lehnert et al. (2003, 2007).

The background $\delta^{13}C$ values from the Kosov section (Fig. 18) are varying roughly between 0‰ and 2.9‰ before the onset of the shift to higher values starts. A similar development is seen in the $\delta^{13}C$ background values in the Mušlovka section, ranging roughly between -0.4‰ and 2‰ with an average value close to 1‰. The background values of $\delta^{13}C$ in the Uddvide-1 core are varying much more gently than those of the Kosov and Mušlovka sections. The $\delta^{13}C$ values from the Kosov section start to rise increasingly from 2.9‰ to 6.7‰ forming a steep rising limb. This rising limb is associated with non-conformity between volcanic tuffitic shales and overlying bioclastic wackestone-packstone, which resemble the development of the rising limb Ronehamn-1 and COG, described above. The onset of the positive $\delta^{13}C$ excursion in the Mušlovka section starts with values of 2.1‰ and 2.8‰. The incomplete plateau of the Kosov section rises slightly from 6.7‰ and reaches a peak value of 8‰. Due to that this deep-water section is cut off by a fault, the $\delta^{13}C$ profile is not complete. The $\delta^{13}C$ values in the Mušlovka section reaches a peak of 4.6‰ before they start to decrease back

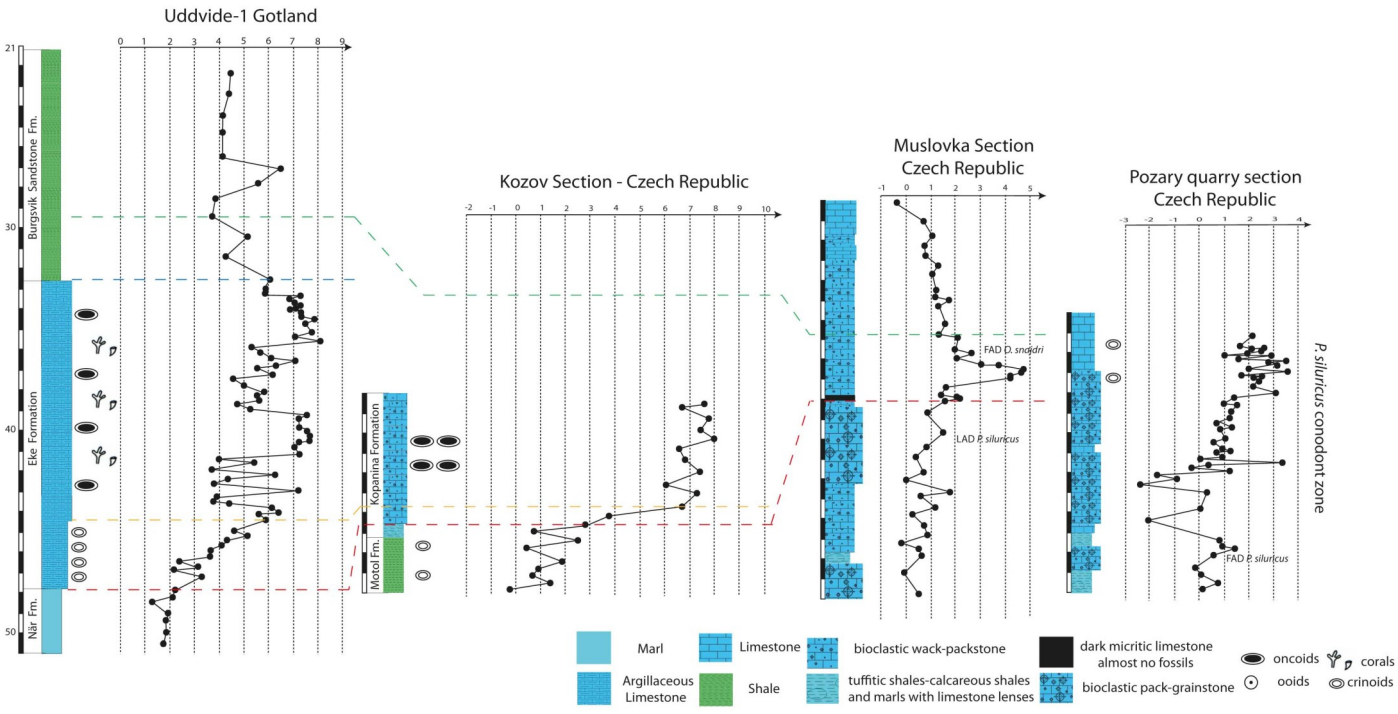

Fig. 18. Chemostratigraphical correlation of the Lau Event between Uddvide-1 Gotland and Peri-Gondowana.

Due to the erosion and/or hiatus in the beds gradually to background values around 1‰. It is worth mentioning that $\delta^{13}C$ values from shallow water sections are higher usually than those of deep water, but the situation is actually the opposite here where $\delta^{13}C$ values from the deep-water Kozov section reach peak values between 6‰ and 8‰, meanwhile the $\delta^{13}C$ peak value of the shallow water Mušlovka section does not exceed 4.6‰. This is interpreted as due to subarerial erosion due to a significant sea-level fall (Lehnert et al. 2007). Due to the erosion and/or hiatus in the beds overlaying the dark micritic limestone layer in Mušlovka section (Manda 2003); we do not have plateau similar to that of Uddvide-1 core section. These two outcrops studied in Prague Basin are accompanied with rapid shift from shaly deeper-water to shallow-water clastic and bioclastic deposits in similar way as in eastern Gotland (Lehnert 2007). It is difficult to correlate $\delta^{13}C$ values of Pozary section, within Prague Basin, with the other sections due to the diagenitic overprint coincides with these values there.

6-2-4 *Uddvide-1, vz. Laurentia*

During the Late Silurian Laurentia was located within a low latitude region facing Gondwana to the south and southwest (Cocks and Scotese, 1991; Golonka et al., 1994; Cocks and Torsvik, 2002; Dalziel, 1997; Niocaill et al., 1997). Data discussed in this section are obtained from Barrick, (2010). The sections studied from Southern Laurentia are located in three places; Oklahoma, Mi-

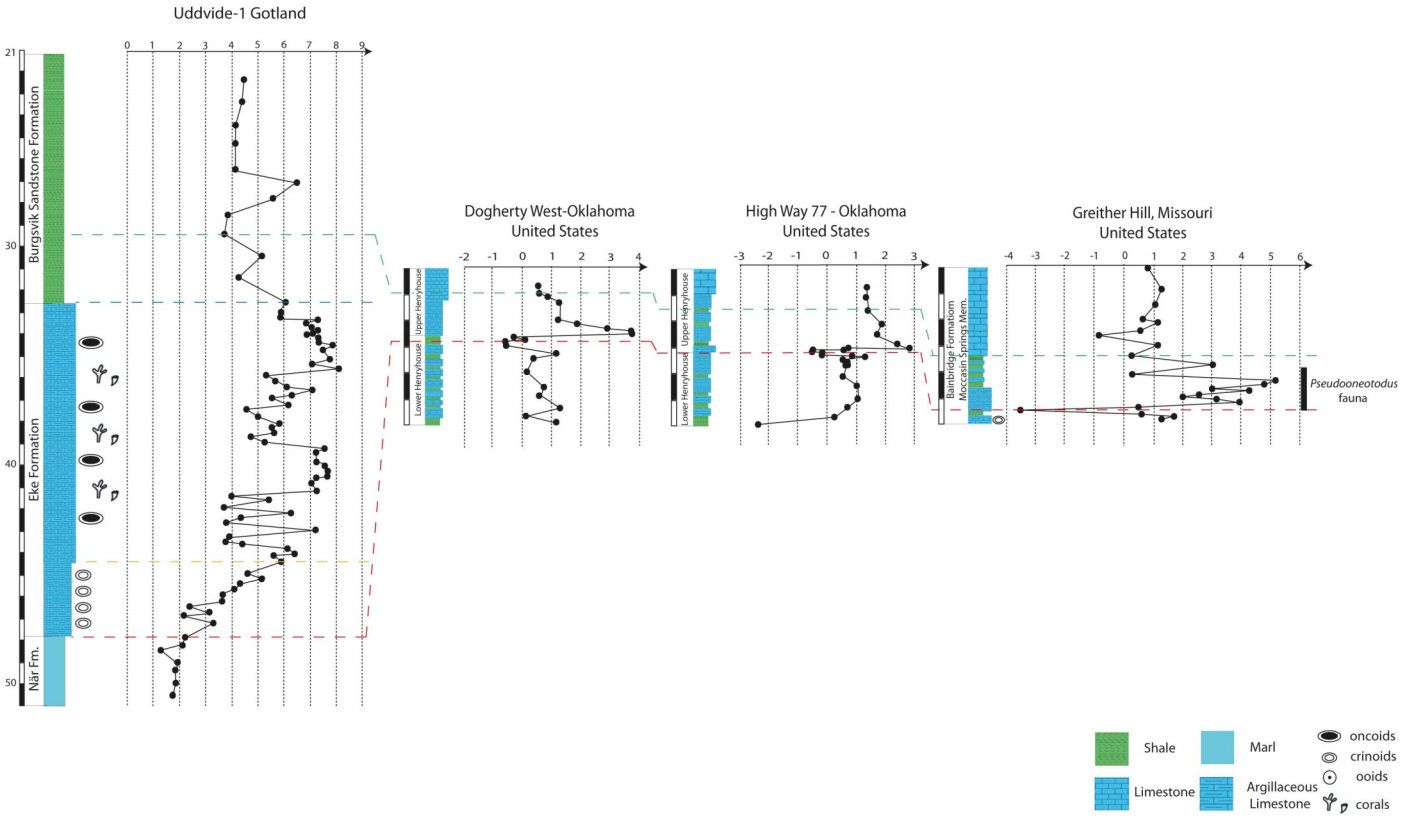

Fig. 19 Chemostratigraphical correlation of the Lau Event between Uddvide-1 Gotland and Laurentia (Oklahoma and Missouri).

ssouri and Tennessee. The Dougherty West-Oklahoma $\delta^{13}C$ profile has background values varying between 0.6‰ and slightly higher than 1‰, with an average baseline of 0.5‰ within the Lower Henry House Member (Fig. 19). The positive shift in $\delta^{13}C$ curve starts at the top of the Lower Henry House Member and is associated with a change in sedimentary facies from argillaceous limestone to calcareous shale an the termination of P. *siluricus*. $\delta^{13}C$ values increase steeply up to 3.5‰ before they start to decline again to slightly above 1‰. They decline to values between 0‰ and 1‰ within the higher portions of the section without forming a plateau similar to that defined in the Uddvide-1 core on Gotland and several other sections from other palaeogeographic regions. The $\delta^{13}C$ curve from the Highway 77 section in Oklahoma shows almost the same trend (Fig. 19). The peak $\delta^{13}C$ value from the Highway 77 section is 2.8‰. Greither Hill-Missouri represents deeper water shelf to basinal facies (Barrick 2010). The background $\delta^{13}C$ values there range between 0.5‰ and 1.5‰ before they fall back to -3.5‰ at the boundary between reddish-colored carbonates and argillaceous shale and limestone accompanied with the termination of P. *siluricus* conodont fauna. $\delta^{13}C$ values increase steeply from -3.5‰ to +4‰ before they form a brief plateau with values fluctuating between 4.1‰ and 5.1‰ with slightly rising trend. $\delta^{13}C$ values decline irregularly to around 1‰ with the appearance of O. *snajdri* conodont fauna. The Linden and Eagle Greek sections in Tennessee seem more similar to the Uddvide-1 core section than to the sections previously described above from Oklahoma and Missouri. The background $\delta^{13}C$ values of the Linden section have base line values of little bit lower than 2‰.

The positive $\delta^{13}C$ shift starts at the top of Beech River Member and seems to coincide with the last appearance datum (LAD) of P. *siluricus* and the occurrence of chert in the section. This shift is increasing gradually from 2‰ up till around 3.63‰ at the boundary between Beech River Member and Bob Member where we have a poorly developed plateau with values rising slightly reaching a peak value of 5.44‰. The notable difference between the plateau of the two sections from Tennessee and the plateau in the Uddvide-1 core section is that the peak value appears early in the plateau in sections of Tennessee, while it appears late in Uddvide-1 core and in similar plateaus of sections from Baltica and Australia before the falling limb starts. The falling limb starts at the upper part of Bob Member where the values decline from 3.57‰ down to around 1‰. The $\delta^{13}C$ curve of Eagle Greek section shows the same trend with very similar $\delta^{13}C$ values except that the background values fluctuate roughly before the onset of the positive shift (Fig. 20), and the plateau seems to start above the boundary between Beech River and Bob Member. The plateau of sections from Tennessee is shorter than those of Gotland, which can be interpreted as lower sedimentation rates in Tennessee as compared to Gotland. The absence of plateau in Oklahoma sections can be interpreted by a major submarine hiatus defined there (Barrick, 2010). The very brief plateau in the Missouri section can be interpreted as that the major marine flooding there took place across somewhat shallower depth. The $\delta^{13}C$ profiles from southern Laurentia are more similar tot hose described from Bohemia which corresp- nds to sediments deposited in deep water settings comparing to those from Gotland and Australia.

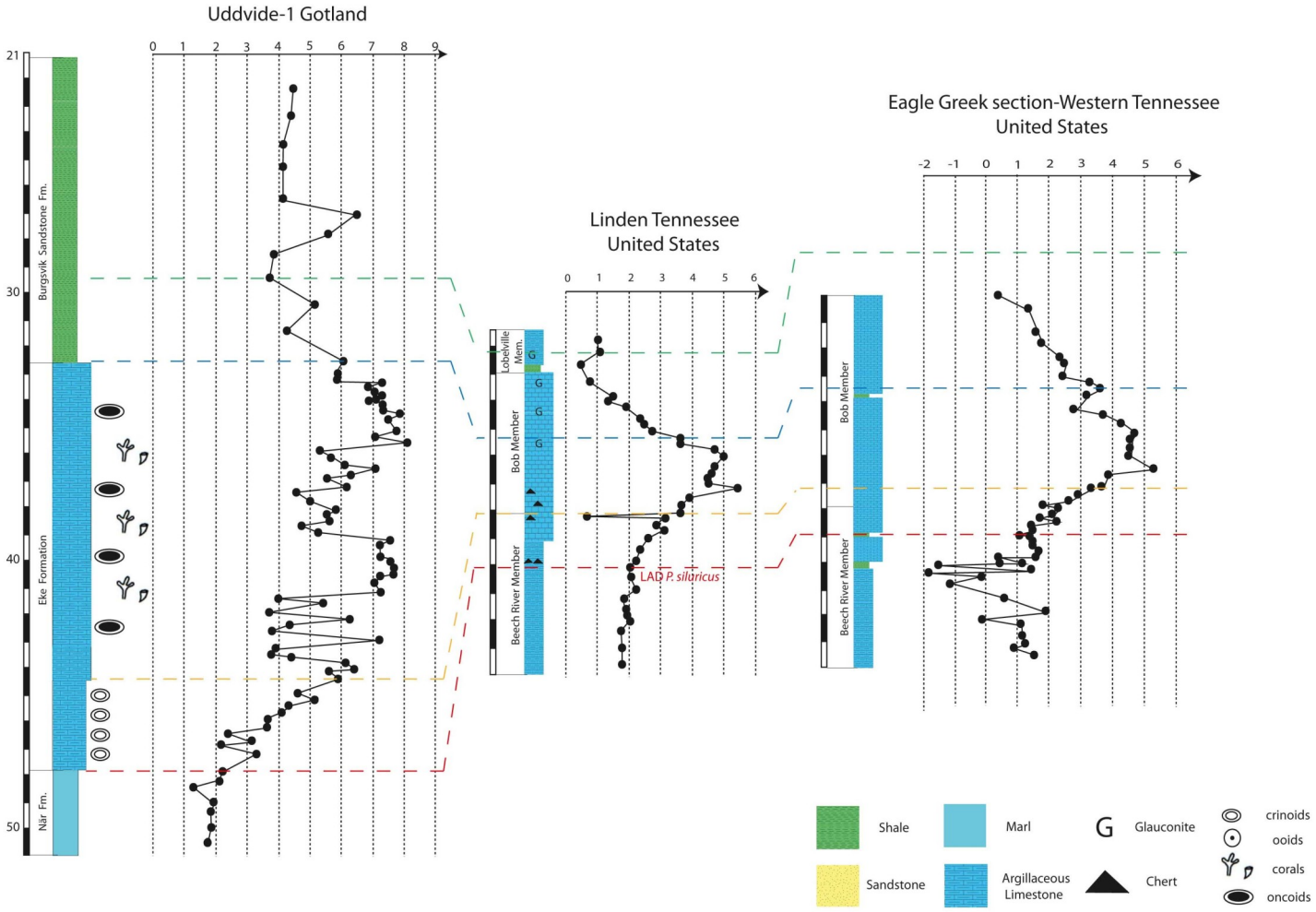

Fig. 20. Chemostratigraphical correlation of the Lau Event between Uddvide-1 Gotland and Laurentia (Tennessee).

7- Conclusions

The Late Silurian Lau Event began at the base of Botvide Member in the uppermost part of the När Formation, Hemse Group, corresponding to the last appearance datum of *P. siluricus*. The event ends at the boundary between the Eke Formation and the lowermost part of the Burgsvik Sandstone, corresponding to the *O. snajdri* conodont zone.

- The turnover of conodonts and other faunas during the Lau Event was accompanied by a prominent positive $\delta^{13}C$ excursion. $\delta^{13}C$ peak values of 9.01‰ and 8.01‰ are documented from the Ronehamn-1 and Uddvide-1 drill cores, respectively.
- The $\delta^{13}C$ profile of the Uddvide-1 drill core spans all stages of and related to the Lau Event in high-resolution. As such, the Uddvide-1 $\delta^{13}C$ profile is a good reference model for correlation with other Lau Event profiles worldwide.
- A contemporaneous regression of sea level can be recognized in studied sections from north-eastern Australia, Peri-Gondwana and Holy Cross Mountains in Southern Baltica, Gotland and Southern Laurentia (Jeppsson et al. 2007; Kozłowski and Munnecke 2010; Lehnert et al. 2007; Calner and Eriksson 2008, Barrick 2010). This contemporaneous regression likely reflect glacio-eustasy. The

beginning of $\delta^{13}C$ rise corresponds with the onset of this regression. This implies that the carbon isotope excursion was accompanied with global change in sea level.

- Anachronistic facies appeared during the event and seem to be globally distributed but at slight different stratigraphic levels. Whereas changes in conodont faunas are closely corresponding between Gotland and COG, they are more difficult to correlate to Laurentia where subdivisions of Icriondontid Zone not have been established. The abundance of these faunas differs between studied palaeo-continents as well.

- Gradually rising limbs of the $\delta^{13}C$ profile correspond to conformable boundaries whereas steeply rising limbs of the $\delta^{13}C$ profile correspond to unconformities with evidence of weathering and/or erosion.

- Large tectonic activity was not recorded in Baltica. The changes in $\delta^{13}C$ are due to rapid sea level changes occurring at the intervals of glacial/interglacial periods.

- Larger positive CIEs correspond to shallow waters at higher latitudes (e.g. Gotland, Queensland) whereas smaller positive CIEs correspond to deeper waters at lower latitudes (e.g. Southern Laurentia, Podolia). This is possibly due to a different nutrient supply, fresh water runoff, turbidity, or changes in ocean circulation. These factors affect the amount of organic ^{13}C sequestered in carbonaceous shells.

8- Acknowledgments:

This project wouldn't be done without cooperation and support of many people. First of all , I would like to acknowledge my supervisors, professor Mikael Calner for all his appreciated efforts in helping, supporting, useful discussions reviewing the manuscript and encouraging me throughout the project and before all for trusting me to implement this project. My assistant supervisor professor Per Ahlberg for the adminstrative support in collaboration with Margretha Kihlbolm. Thanks to my external supervisor professor Oliver Lehnert for the chemostratigraphical analyses. Special thanks to professor Mats Eriksson for the valueable field trip to Gotland. Deep acknowledgmnts to professors Ulf Söderlund and Anders Scherstén for their appreciated support and encouraging to continue the full Master's Degree at Lund University. Full appreciaition and many thanks for all those great teachers who have taught me at both Geology Department in Lund University and Damascus University. Thanks for Erasmus Mundus for financing the most part of my study here. Many thanks for both people and government of Sweden for the nice hospitality. Warm thanks to my family, my great mother Sanaa, and my friends who have supported me in the most critical and hard instances. Last and not least, all the respect and gratitude for the brave and great people of Syria who inspired me a lot to go on.

9- References:

Baarli, B.G. Johnson, M.E. and Antoshkina, A.I. (2003). Silurian stratigraphy and Paleogeography of Baltica. In: Landing E, Johnson ME (eds) Silurian lands and seas, Paleogeography outside of Laurentia. *New York State Museume Bulletin, New York, 492*, 3-34.

Barrick, J.E. Kleffner M.A. Gibson, M.A. Peavey F.N. and Karlsson H.A. (2010). The min-Ludfordian Lau event and Carbon Isotope Excursion (Ludlow, Silurian) in southern Laurentia- Preliminary Results. Bollettino della società Paleontologica Italiana,, 49(1), 13-33.

Bergstrom, S.M. Saltzman, M. and Schmitz, B. (2006). First record of the Hirnantian (Upper Ordovician) delta (super 13) C excursion in the North American Midcontinent and its regional implications. *Cambridge University Press, London, United Kingdom, 143*, 657-678.

Bopp, L. and Le Quere, C. (2009). Ocean carbon cycle. *American Geophysical Union, Washington, DC, United States, 187*, 181-195.

Bosence, Dan.W.J. Wilson, R. and Chris L. (2003). Carbonate depositional system: in The sedimentary record of sea-level change Coe, A. L. *press syndicate of the university of Cambridge*, 209-233.

Brenchley, P.J. Carden, G. A. Hints, L. kaljio, D. Marshall, J.D. Martma, T. Meidla, T. and Nŏlvak, J. (2003). High resolution isotope stratigraphy of Late Ordovician sequences: constraints on the timing of bioevents and environmental changes associated with mass extinction and glaciation. *geological Society of America Bulletin, 115*, 89-104.

Calner, M. Kozłowska, A. Masiak, M. and Schmitz, B. *(*2006). A shoreline to deep basin correlation chart for the middle Silurian coupled extinction-stable isotope event. *GFF, 128*, 79-84.

Calner, M. J. (2004). The Silurian of Gotland- Part I: Review of the stratigraphic framework, event stratigraphy, and stable carbon and oxygen isotope develoment. *Erlangen Geologische Abhandlungen., 5*, 113-131.

Calner, M. (2005). A Late Silurian extinction event and anachronistic period. *Geology, 33*, 305-308.

Calner, M. and Eriksson, M.J. (2006). Evidence for rapid environmental change in low latitude during the Late Silurian Lau Event: the Burgen-1 drillcore, Gotland, sweden. *Geological magazine, 143*, 15-24.

Calner, M. (2008). Silurian global events- at the tipping point of climate change. *In Elewa A.M.T. (ed), Mass Extinction, Springer*, 21-57.

Calner, M. and Eriksson, M.E. 2012. Microbially induced sedimentary structures (MISS) from the Palaeozoic of Sweden. *Society of Economic Paleontologist and Mineralogist*, special volume. In press.

Cocks, L.R.M. and Scotese, C.R. (1991). The global paleogeography of the Silurian Period. *The Palaeontological Association, Special Papers in Paleontology, 44*, 109-122.

Cocks, L.R.M. and Torsvik, T.H. (2002). Earth geography from 500 to 400 million years ago: a faunal and paleomagnetic review. *Journal of the Geological Society, London*, volume 159, 631-644.

Coe, A. L. and Church K. D. (2003). Sea-level change in: The sedimentary record of sea-level change Coe, A. L. *Press syndicate of the university of Cambridge*, 34-56.

Coleman, D. C. and Fry, B. Boutton, T.W. Ehleringer, J.R. (1991). Carbon isotope techniques. *Academic press, INC San Deigo,*

California, USA, 155-200.

Cramer, B. D. and Saltzman, M. R. (2006). The late Wenlock Mulde positive carbon isotope excursion in North America. *GFF, 128*, 85-90.

Cramer, B. D, Kleffner, M. A. and Saltzman, M. R. (2005). Sequestration of 12C in the deep ocean during the early Wenlock (Silurian) positive carbon isotope excursion. *Palaeogeogr Palaeoclimatol Palaeoecol, 219*, 333-349.

Dalziel, I.W.D. (1997). Neoproterozoic geography and tectonics: Review, hypothesis, environment speculation. *Geological Society of America Bulletin, 109*, 16-42.

Dawson, T.E. and Siegwolf R.T.W. (2007). Stable isotopes as indicators of ecological change. *Elsivier USA*.

Eriksson, M. Bergman, C.F. Jeppsson, L. (2004). Review of Palaeobotany and Palynology: Silurian scolecodonts. *Elsevier, Amsterdam, 131*, 269–300.

Eriksson, M.J. Calner, M. (2008). A sequence stratigraphical model for the Late Ludfordian (Silurian) of Gotland, Sweden: implications for timing between changes in sea level, palaeoecology, and the global carbon cycle. *Facies, 54*, 253-276.

Golonka, J.M. Ross, M.I. and Scotese, C.R. (1994). Phanerozoic paleogeographic and paleoclimatic modeling maps. *In Embry A.F., Beauchamp B. and Glass D.J. (eds), pangea: Global Environments and Resources. canadian Society of Petroleum Geologists Memoir, 17*, 1-47.

Hagadorn, J.W. and Bottjer, D.J. (1997). Wrinkle structures: microbially mediated sedimentary structures common in subtidal siliclastic settings at the Proteozoic-Phanerozoic transition. *Geology, 25*, 1047-1050.

Hede, .E. (1960). The Silurian of Gotland. in G. Regnèll and J :E. Hede (eds.): The Lower Palaeozoic of Scania. The Silurian of Gotland. *International Geological Congress*

XXI. Session Norden. Guidebook sweden d. Stockholm. Publications of the Institute of Mineralogy, Palaeontology and Quaternary Geology of the University of Lund 91.

Jeppsson, L. (1998). Silurian oceanic events: summary of general charchteristics: Landing, E., Johnson, M.E. (Eds.), Silurian Cycles: Linkages of Dynamic Stratigraphy with Atmospheric, Oceanic, and Tectonic Changes (James Hall Centennial Volume). *New York State Museum Bulletin, 491*, 239-257.

Jeppsson, L. and Calner, M. (2003). The Silurian Mulde Event and a scenario forsecundo-secundo events. *Royal Society of Edinburgh Transactions, Earth Sciences, 93*, 135-154.

Jeppsson, L. and Aldridge, R.J. (2000). Ludlow (Late Silurian) oceanic episodes and events. *J Geol Soc Lond*, 1137-1148.

Jeppsson, L. Eriksson, M.E. and Calner, M. (2005). Conodont-based revisions of the Late Ludfordian on Gotland, Sweden. *GFF, 127*, 273 -282.

Jeppsson, L. Eriksson M.E. and Calner, M. (2006). A Latest Llandovery to latest Ludlow high-resolution biostratigraphy based on the Silurian of Gotland-a summery. *GFF, 128*, 109-114.

Jeppsson, L. talent, J.A. Mawson, R. Simpson, A.J. Andrew, A. Calner, M. Whitford, D. Trotter, J.A. Sandström, O. Caldon, H.J. (2007). High-resolution Late Silurian correlations between Gotland, Sweden, and the Broken River region, NE Australi: lithologies, conodonts and isotopes. *Palaeogeogr Palaeoclimatol Palaeoecol, 245*, 115-137.

Jeppsson, L. (1987). Lithological and conodont distributional evidence for episodes of anomalous oceanic conditions during the Silurian. in Palaeobiology (ed. R. J. Aldridge).

British Micropaleontological Society series., 129-45.

Jeppsson, L. (1990). An oceanic model for lithoöogical and faunal changes tested on the Silurian record. *Journal of the Geological Society, London, 147*, 663-674.

Jeppsson, L. (1993). Silurian events: the theory and the conodonts. *Proceedings of the Estonian Academy of Sciences, Geology 42*, 23-27.

Jeppsson, L. (1998). Silurian oceanic events: Summary of general characteristics In Landing E.and Johnson M.E. (eds), Silurian cycles: Linkages of dynamic stratigraphy with atmospheric, oceanic, and tectonic changes. *New York State Museume Bulletin, New York, 491*, 239-257.

Kaljio, D. Grytsenko, V. Martma, T. and Motus, M.A. (2007). Three global carbon isotope shifts in the Silurian of Podolia (Ukraine): stratigraphic implications. *Estonian Journal of Earth Sciences, 56*, 205-220.

Kozłowski. W. and Munnecke, A (2010). Stable carbon isotope development and sea-level changes during the Late Ludlow (Silurian) of the Łysogóry region (Rzepin section, Holy Mountains, Poland). *Facies, 56*, 615-633.

Lehnert, O. Fryda, J. Buggisch, W. Munnecke, A. and Manda, S. (2003). A first report of the Ludlow Lau event from the Prague Basin (Barrandian, Czech Republic). *INSUGEO serie correlación Geológica, 18*, 139-44.

Lehnert, O. Fryda, J. Buggisch, W. Munnecke, A. Nützel, A. Kriz, J. and Manda, S. (2007). δ13C records across the Late Silurian Lau Event: new data from middle paleolatitudes of northern peri-Gondwana. *palaeogeography, palaeoclimatology, Palaeoecology, 245*, 227-244.

Lehnert, O. Joachimski, M. Buggisch, W. Stouge, S. Fryda, J. Jeppsson, L. (2006). Two case studies on early Palaeozoic climate reconstructions based on delta (super ^{18} O) data from conodont apatite; an Early to Mid-Ordovician greenhouse and Late Silurian icehouse. *International conodont symposium*, 52.

Lehnert, O. Mannik, P. Joachimski, M. Calner, M. Fryda, J. (2010). Palaeoclimate perturbations before the Sheinwoodian glaciation; a trigger for extinctions during the "Ireviken event". *Palaeogeography, Palaeoclimatology, Palaeoecology, 296*, 320-331.

Longhurst, A. R. (1991). Role of the marine biosphere in the global carbon cycle. *Limnology and Oceanography, 36*, 1507-1526.

Manda, S. (2003). Vŷvoj a Společenstva silurskŷch a rannè devonskŷch hlavonožcovŷch vápencu (pražska pánev, Čechy). in Lehnert, O. et al, 2007. *Unpublished Diploma thesis; MS Přirodovèdecká fakulta, Universita Karlova, Praha*, 114 and supplement I-XIV.

Manten, A. (1971) 13. Silurian reefs of Gotland. Developments in sedimentology. *Elsevier, Amsterdam*.

Munnecke, A. Samtleben, C. and Bickert, T. (2003). The Ireviken Event in the lower Silurian of Gotland, Sweden-relation to similar palaeozoic and Proterozoic events. *Palaegeography, palaeoclimatology, Palaeoecology, 195*, 99-124.

Myro, P.M. Tiece, L. Archuleta, B. Clark, B. Taylor, J.F. and Ripperdan, R.L. (2004). Flat-Pepple conglomerate: its multiple origins and relationships to metre-scale depositional cycle. *Sedimentology, 51*, 973-96.

Niocaill, C.B.M. van der Pluijim, B.A. and van der Voo, R. (1997). Ordovician paleogeography and the evolution of the Iapetus Ocean. *Geology, 25*, 159-162.

Poprawa, P. Sliaupa, S. Stephenson, R. Lazauskiene, J. (1999). Late Vendian-early Palaeozoic tectonic evolution of the Baltic Basin: regional tectonic implications from subsidence analysis. Tectonophysics, 314, 219.239.

Pruss, S. Fraiser, M. Bottjer, D.J. (2004). Proliferation of early Triassic wrinkle structures: implications for environmental stress following the end-Permian mass extinction. Geology, 32, 461-464.

Saltzman, M.R. (2001). Silurian δ13C stratigraphy: A view from North America. *Geology, 29*, 671-674.

Samtleben, C. Munnecke, A. and Bickert, T. (2000). Development of facies and C/O-isotopes in transects through the Ludlow of Gotland: Evidence for global and local influences on a shallow-marine environment. *Facies, 43*, 1-38.

Scheehan, P. M. and Harris, M. T. (2004). Microbialite resurgence after the Late Ordovician extinction. *Nature, 430*, 75-7.

Schubert, J. K. and Bottjer, D. J. (1992). Early Triassic stromatolites as post-mass extinction disaster forms. *Geology, 20*, 883-886.

Sepkoski, J.J.Jr. (1982). Flat-Pebble conglomerates, storm deposits, and the Cambrian bottom fauna, in Einsele, G., and Seilacher, A., eds., Cyclic and event stratification. *Spinger -Verlag*, 371-385.

Stricanne, L. Munnecke, A. and Pross, J. (2006). Assessing mechanism of environmental change: Palynological signals across the Late Ludlow (Silurian) positive isotope excursion (δ13C, δ18 O) on Gotland, Sweden. *Palaeogeography, Palaeoclimatology, Palaeoecology*, 230, 1-31.

Cocks, L.R.M. and Torsvik, T.H. (2002). Earth geography from 500 to 400 million years ago: a faunal and paleomagnetic review. Journal of the Geological Society, London, 159, 631-644.

Whalen, M.T. Day, J. Eberli, G.P. and Homewood, P.W. (2002). Microbial carbonates s indicators of environmental change and biotic crises in carbonate systems: examples from Late Devonian, Alberta basin, Canada.Microbial carbonates s indicators of environmental change and biotic crises in carbonate systems: examples. Palaeogeography, palaeoclimatology, Palaeoecology, 181, 127-51.

Wigforss-Lange, J. (1999). Carbon isotope ^{13}C enrichment in upper silurian (Whitecliffian) marine calcareous rocks in Scania, Sweden. *GFF, 121*, 273-279.

Wenzel, B. Joachimski, M.M. (1996). Carbon and oxygen isotopic composition of Silurian brachiopods (Gotland/Sweden); palaeoceanographic implications. *Palaeogeography, Palaeoclimatology, Palaeoecology*, 122, 1-4, 143-166.

10- Appendix

Appendix A: Table. 2 $\delta^{13}C$ data of Uddvide-1 drill core samples.

Appendix B: Table. 2 $\delta^{13}C$ data of Ronehamn-1 drill core samples.

Appendix C: Figure 15. Chemostratigraphical correlation of the Lau Event on different palaeocontinents.

Appendix A: Table. 2 $\delta^{13}C$ data of Uddvide-1 drill core samples.

Identifier	Formation	Depth (m)	$\delta^{13}C$	Identifier	Formation	Depth (m)	$\delta^{13}C$
U1	När Formation	-60.84	0.74	U48	Eke Formation	-41.09	7.21
U2	När Formation	-60.19	0.71	U49	Eke Formation	-40.74	6.99
U3	När Formation	-59.13	1.00	U50	Eke Formation	-40.47	7.17
U4	När Formation	-58.20	1.34	U51	Eke Formation	-40.32	7.59
U5	När Formation	-57.17	0.62	U52	Eke Formation	-40.20	7.59
U6	När Formation	-56.18	0.87	U53	Eke Formation	-39.98	7.50
U7	När Formation	-55.03	0.66	U57	Eke Formation	-39.95	5.20
U8	När Formation	-54.23	1.65	U54	Eke Formation	-39.80	7.18
U9	När Formation	-53.21	1.42	U55	Eke Formation	-39.44	7.16
U10	När Formation	-53.07	0.86	U56	Eke Formation	-39.30	7.43
U11	När Formation	-52.21	1.68	U58	Eke Formation	-38.66	4.62
U12	När Formation	-51.73	1.51	U59	Eke Formation	-38.38	5.51
U13	När Formation	-51.17	1.28	U63	Eke Formation	-38.19	4.46
U14	När Formation	-50.90	0.69	U62	Eke Formation	-37.93	4.92
U15	När Formation	-50.34	1.67	U61	Eke Formation	-37.69	5.74
U16	När Formation	-49.82	1.80	U60	Eke Formation	-37.45	5.44
U17	När Formation	-49.26	1.77	U63	Eke Formation	-37.26	6.09
U18	När Formation	-48.93	1.85	U64	Eke Formation	-36.94	5.48
U19	När Formation	-48.23	1.18	U65	Eke Formation	-36.75	6.27
U20	När Formation	-48.01	2.02	U66	Eke Formation	-36.54	7.07
U21	Eke Formation	-47.61	2.25	U67	Eke Formation	-36.32	6.07
U22	Eke Formation	-47.05	3.22	U68	Eke Formation	-36.10	5.75
U23	Eke Formation	-46.77	2.09	U69	Eke Formation	-35.75	5.20
U24	Eke Formation	-46.51	3.09	U70	Eke Formation	-35.58	8.03
U25	Eke Formation	-46.25	2.59	U71	Eke Formation	-35.38	7.08
U26	Eke Formation	-46.14	3.56	U72	Eke Formation	-35.03	7.68
U27	Eke Formation	-45.84	3.60	U73	Eke Formation	-34.70	7.44
U28	Eke Formation	-45.62	4.06	U74	Eke Formation	-34.51	7.73
U29	Eke Formation	-45.32	4.20	U75	Eke Formation	-34.43	7.22
U31	Eke Formation	-45.07	5.10	U76	Eke Formation	-34.06	7.21
U32	Eke Formation	-44.80	4.50	U77	Eke Formation	-33.90	6.78
U33	Eke Formation	-44.63	5.92	U78	Eke Formation	-33.66	7.04
U34	Eke Formation	-44.50	5.46	U79(1)	Eke Formation	-33.53	7.20
U36	Eke Formation	-44.06	6.31	U79(2)	Eke Formation	-33.47	6.94
U37	Eke Formation	-43.80	6.11	U80	Eke Formation	-33.23	6.74
U38	Eke Formation	-43.47	4.31	U81	Eke Formation	-33.02	7.17
U39	Eke Formation	-43.26	3.73	U82	Eke Formation	-32.87	5.77
U40	Eke Formation	-43.16	3.84	U83	Eke Formation	-32.67	5.78
U41	Eke Formation	-42.82	7.15	U84	Burgsvik Sandstone	-32.27	6.05
U42	Eke Formation	-42.54	3.73	U85	Burgsvik Sandstone	-31.03	4.20
U43	Eke Formation	-42.29	4.52	U86	Burgsvik Sandstone	-29.95	5.08
U44	Eke Formation	-42.11	6.18	U87	Burgsvik Sandstone	-29.11	3.65
U45	Eke Formation	-41.81	3.63	U88	Burgsvik Sandstone	-28.12	3.73
U46	Eke Formation	-41.68	5.28	U89	Burgsvik Sandstone	-27.28	5.51
U47	Eke Formation	-41.35	3.89	U90	Burgsvik Sandstone	-26.63	6.44

Identifier	Formation	Depth (m)	$\delta^{13}C$	Identifier	Formation	Depth (m)	$\delta^{13}C$
U91	Burgsvik Sandstone	-26.05	4.10	U106	Burgsvik Sandstone	-11.89	3.21
U92	Burgsvik Sandstone	-24.98	4.02	U107	Burgsvik Sandstone	-10.94	4.12
U93	Burgsvik Sandstone	-23.98	4.13	U110	Burgsvik Sandstone	-8.12	3.86
U94	Burgsvik Sandstone	-23.10	4.27	U111	Burgsvik Sandstone	-7.12	3.90
U95	Burgsvik Sandstone	-22.00	4.39	U112	Burgsvik Sandstone	-6.11	3.76
U96	Burgsvik Sandstone	-21.04	0.09	U113	Burgsvik Sandstone	-5.09	4.00
U97	Burgsvik Sandstone	-20.05	3.72	U114	Burgsvik Sandstone	-4.01	3.58
U98	Burgsvik Sandstone	-19.13	3.29	U115	Burgsvik Sandstone	-3.18	3.62
U99	Burgsvik Sandstone	-18.02	3.89	U116	Burgsvik Sandstone	-2.03	4.03
U100	Burgsvik Sandstone	-16.98	3.71	U117	Burgsvik Sandstone	-1.12	5.57
U101	Burgsvik Sandstone	-16.07	4.12	U118	Burgsvik Sandstone	-0.84	5.97
U102	Burgsvik Sandstone	-15.12	3.93	U119	Burgsvik Oolite	0.12	6.64
U103	Burgsvik Sandstone	-14.38	2.97	U120	Burgsvik Oolite	0.40	7.48
U104	Burgsvik Sandstone	-13.80	4.04	U121	Burgsvik Oolite	0.67	7.45
U105	Burgsvik Sandstone	-12.92	3.72				

Appendix B: Table. 3 $\delta^{13}C$ data of Ronehamn-1drill core samples.

Identifier	Formation	Depth (m)	$\delta^{13}C$	Identifier	Formation	Depth (m)	$\delta^{13}C$
R 1	När Formation	-26.71	1.40	R 30	Eke Fo. (Crinoidal zone)	-11.48	5.19
R 2	När Formation	-25.62	1.35	R 31	Eke Fo. (Crinoidal zone)	-11.25	5.42
R 3	När Formation	-24.64	0.36	R 32	Eke Fo. (Crinoidal zone)	-10.97	5.06
R 4	När Formation	-23.62	1.19	R 33	Eke Formation	-10.75	5.63
R 5	När Formation	-22.64	0.94	R 34	Eke Formation	-10.52	5.68
R 6	När Formation	-21.82	1.17	R 35	Eke Formation	-10.26	4.44
R 7	När Formation	-21.00	0.94	R 36	Eke Formation	-10.00	6.82
R 8	När Formation	-20.48	1.52	R 37	Eke Formation	-9.76	6.07
R 9	När Formation	-20.00	1.66	R 38	Eke Formation	-9.51	5.19
R 10	När Formation	-19.44	0.91	R 39	Eke Formation	-9.24	4.01
R 11	När Formation	-18.98	1.37	R 40	Eke Formation	-9.00	4.68
R 12	När Formation	-18.50	1.49	R 41	Eke Formation	-8.78	3.53
R 13	När Formation	-18.02	1.36	R 43	Eke Formation	-8.24	4.18
R 14	När Formation	-17.42	0.93	R 44	Eke Formation	-7.88	3.51
R 15	När Formation	-17.20	1.68	R 45	Eke Formation	-7.77	7.67
R 16	När Formation	-16.72	1.52	R 46	Eke Formation	-7.75	4.18
R 17	När Formation	-16.09	1.71	R 47	Eke Formation	-7.51	7.42
R 18	När Formation	-15.63	1.33	R 48	Eke Formation	-7.25	7.46
R 19	När Formation	-15.11	1.18	R 49	Eke Formation	-7.01	7.41
R 20	När Formation	-14.60	1.07	R 50	Eke Formation	-6.75	7.57
R 21	När Formation	-14.20	1.83	R 51	Eke Formation	-6.49	7.99
R 22	När Formation	-13.52	0.91	R 52	Eke Formation	-6.21	5.54
R 23	När Formation	-13.27	1.05	R 53	Eke Formation	-6.03	7.54
R 24	När Formation	-13.00	1.08	R 54	Eke Formation	-5.89	7.27
R 25	När Formation	-12.75	2.00	R 55	Eke Formation	-5.48	5.63
R 26	När Fo. (Botvide Memmber)	-12.63	1.83	R 56	Eke Formation	-5.20	7.50
R 27	När Fo. (Botvide Memmber)	-12.28	3.47	R 57	Eke Formation	-4.98	7.15
R 28	När Fo. (Botvide Memmber)	-11.98	5.06	R 58	Eke Formation	-4.75	6.37
R 29	Eke Fo. (Crinoidal zone)	-11.73	4.99	R 59	Eke Formation	-4.51	7.01

Identifier	Formation	Depth (m)	$\delta^{13}C$	Identifier	Formation	Depth (m)	$\delta^{13}C$
R 60	Eke Formation	-4.26	4.51	R 72	Eke Formation	-1.31	8.92
R 61	Eke Formation	-3.98	5.84	R 73	Eke Formation	-1.00	8.58
R 62	Eke Formation	-3.73	7.88	R 74	Eke Formation	-0.81	8.92
R 63	Eke Formation	-3.48	7.99	R 75	Eke Formation	-0.42	8.24
R 64	Eke Formation	-3.22	7.82	R 76	Eke Formation	-0.18	6.40
R 65	Eke Formation	-2.95	8.01	R 77	Eke Formation	-0.13	8.03
R 66	Eke Formation	-2.72	5.57	R 78	Burgsvik Sandstone	0.06	5.60
R 67	Eke Formation	-2.47	8.40	R 79	Burgsvik Sandstone	0.29	8.08
R 68	Eke Formation	-2.20	7.59	R 80	Burgsvik Sandstone	0.54	7.11
R 69	Eke Formation	-2.01	9.01	R 81	Burgsvik Sandstone	0.78	5.06
R 70	Eke Formation	-1.75	8.70	R 82	Burgsvik Sandstone	1.02	7.51
R 71	Eke Formation	-1.45	8.61	R 83	Burgsvik Sandstone	1.27	5.98

Tidigare skrifter i serien ”Examensarbeten i Geologi vid Lunds Universitet”:

269. Dyck, Brendan, 2010: Metamorphic rocks in a section across a Svecnorwegian eclogite-bearing deformation zone in Halland: characteristics and regional context. (15 hp)
270. McGimpsey, Ian, 2010: Petrology and lithogeochemistry of the host rocks to the Nautanen Cu-Au deposit, Gällivare area, northern Sweden. (45 hp)
271. Ulmius, Jan, 2010: Microspherules from the lowermost Ordovician in Scania, Sweden – affinity and taphonomy. (15 hp)
272. Andersson, Josefin, Hybertsen, Frida, 2010: Geologi i Helsingborgs kommun – en geoturistkarta med beskrivning. (15 hp)
273. Barth, Kilian, 2011: Late Weichselian glacial and geomorphological reconstruction of South-Western Scania, Sweden. (45 hp)
274. Mashramah, Yaser, 2011: Maturity of kerogen, petroleum generation and the application of fossils and organic matter for paleotemperature measurements. (45 hp)
275. Vang, Ina, 2011: Amphibolites, structures and metamorphism on Flekkerøy, south Norway. (45 hp)
276. Lindvall, Hanna, 2011: A multi-proxy study of a peat sequence on Nightingale Island, South Atlantic. (45 hp)
277. Bjerg, Benjamin, 2011: Metodik för att förhindra metanemissioner från avfallsdeponier, tillämpad vid Albäcksdeponin, Trelleborg. (30 hp)
278. Pettersson, Hanna, 2011: El Hicha – en studie av saltstäppssediment. (15 hskp)
279. Dyck, Brendan, 2011: A key fold structure within a Sveconorwegian eclogite-bearing deformation zone in Halland, south-western Sweden: geometry and tectonic implications. (45 hp)
280. Hansson, Anton, 2011: Torvstratigrafisk studie av en trädstamshorisont i Viss mosse, centrala Skåne kring 4 000 - 3 000 cal BP med avseende på klimat- och vattenståndsförändringar. (15 hp)
281. Åkesson, Christine, 2011: Vegetationsutvecklingen i nordvästra Europa under Eem och Weichsel, samt en fallstudie av en submorän, organisk avlagring i Bellinga stenbrott, Skåne. (15 hp)
282. Silveira, Eduardo M., 2011: First precise U-Pb ages of mafic dykes from the São Francisco Craton. (45 hp)
283. Holm, Johanna, 2011**:** Geofysisk utvärdering av grundvattenskydd mellan väg 11 och Vombs vattenverk. (15 hp)
284. Löfgren, Anneli, 2011: Undersökning av geofysiska metoders användbarhet vid kontroll av den omättade zonen i en infiltrationsdamm vid Vombverket. (15 hp)
285. Grenholm, Mikael, 2011: Petrology of Birimian granitoids in southern Ghana - petrography and petrogenesis. (15 hp)
286. Thorbergsson, Gunnlaugur, 2011: A sedimentological study on the formation of a hummocky moraine at Törnåkra in Småland, southern Sweden. (45 hp)
287. Lindskog, Anders, 2011: A Russian record of a Middle Ordovician meteorite shower: Extraterrestrial chromite in Volkhovian-Kundan (lower Darriwilian) strata at Lynna River, St. Petersburg region. (45 hp)
288. Gren, Johan, 2011: Dental histology of Cretaceous mosasaurs (Reptilia, Squamata): incremental growth lines in dentine and implications for tooth replacement. (45 hp)
289. Cederberg, Julia, 2011: U-Pb baddelyit dateringar av basiska gångar längs Romeleåsen i Skåne och deras påverkan av plastisk deformation i Protoginzonen (15 hp)
290. Ning, Wenxing, 2011: Testing the hypothesis of a link between Earth’s magnetic field and climate change: a case study from southern Sweden focusing on the 1st millennium BC. (45 hp)
291. Holm Östergaard, Sören, 2011: Hydrogeology and groundwater regime of the Stanford Aquifer, South Africa. (45 hp)
292. Tebi, Magnus Asiboh, 2011: Metamorphosed and partially molten hydrothermal alteration zones of the Akulleq glacier area, Paamiut gold province, South-West Greenland. (45 hp)
293. Lewerentz, Alexander, 2011: Experimental zircon alteration and baddeleyite formation in silica saturated systems: implications for dating hydrothermal events. (45 hp)
294. Flodhammar, Ingrid, 2011: Lövestads åsar:

En isälvsavlagring bildad vid inlandsisens kant i Weichsels slutskede. (15 hp)

295. Liu, Tianzhuo, 2012: Exploring long-term trends in hypoxia (oxygen depletion) in Western Gotland Basin, the Baltic Sea. (45 hp)
296. Samer, Bou Daher, 2012: Lithofacies analysis and heterogeneity study of the subsurface Rhaetian–Pliensbachian sequence in SW Skåne and Denmark. (45 hp)
297. Riebe, My, 2012: Cosmic ray tracks in chondritic material with focus on silicate mineral inclusions in chromite. (45 hp)
298. Hjulström, Joakim, 2012: Återfyllning av borrhål i geoenergisystem: konventioner, metod och material. (15 hp)
299. Letellier, Mattias, 2012: A practical assessment of frequency electromagnetic inversion in a near surface geological environment. (15 hp)
300. Lindenbaum, Johan, 2012: Identification of sources of ammonium in groundwater using stable nitrogen and boron isotopes in Nam Du, Hanoi. (45 hp)
301. Andersson, Josefin, 2012: Karaktärisering av arsenikförorening i matjordsprofiler kring Klippans Läderfabrik. (45 hp)
302. Lumetzberger, Mikael, 2012: Hydrogeologisk kartläggning av infiltrationsvattentransport genom resistivitetsmätningar. (15 hp)
303. Martin, Ellinor, 2012: Fossil pigments and pigment organelles – colouration in deep time. (15 hp)
304. Rådman, Johan, 2012: Sällsynta jordartsmetaller i tungsand vid Haväng på Österlen. (15 hp)
305. Karlstedt, Filippa, 2012: Jämförande geokemisk studie med portabel XRF av obehandlade och sågade ytor, samt pulver av Karlshamnsdiabas. (15 hp)
306. Lundberg, Frans, 2012: Den senkambriska alunskiffern i Västergötland – utbredning, mäktigheter och faciestyper. (15 hp)
307. Thulin Olander, Henric, 2012: Hydrogeologisk kartering av grundvattenmagasinet Ekenäs-Kvarndammen, Jönköpings län. (15 hp)
308. Demirer, Kursad, 2012: U-Pb baddeleyite ages from mafic dyke swarms in Dharwar craton, India – links to an ancient supercontinent. (45 hp)
309. Leskelä, Jari, 2012: Loggning och återfyllning av borrhål – Praktiska försök och utveckling av täthetskontroll i fält. (15 hp)
310. Eriksson, Magnus, 2012: Stratigraphy, facies and depositional history of the Colonus Shale Trough, Skåne, southern Sweden. (45 hp)
311. Larsson, Amie, 2012: Kartläggning, beskrivning och analys av Kalmar läns regionalt viktiga vattenresurser. (15 hp)
312. Olsson, Håkan, 2012: Prediction of the degree of thermal breakdown of limestone: A case study of the Upper Ordovician Boda Limestone, Siljan district, central Sweden. (45 hp)
313. Kampmann, Tobias Christoph, 2012: U-Pb geochronology and paleomagnetism of the Westerberg sill, Kaapvaal Craton – support for a coherent Kaapvaal-Pilbara block (Vaalbara). (45 hp)
314. Eliasson, Isabelle Timms, 2012: Arsenik: förekomst, miljö och hälsoeffekter. (15 hp)
315. Badawy, Ahmed Salah, 2012: Sequence stratigraphy, palynology and biostratigraphy across the Ordovician-Silurian boundary in the Röstånga-1 core, southern Sweden. (45 hp)
316. Knut, Anna, 2012: Resistivitets- och IP-mätningar på Flishultsdeponin för lokalisering av grundvattenytor. (15 hp)
317. Nylén, Fredrik, 2012: Förädling av ballastmaterial med hydrocyklon, ett fungerande alternativ? (15 hp)
318. Younes, Hani, 2012: Carbon isotope chemostratigraphy of the Late Silurian Lau Event, Gotland, Sweden. (45 hp)

LUNDS UNIVERSITET

Geologiska institutionen
Lunds universitet
Sölvegatan 12, 223 62 Lund